YTTRIUM OXIDE: A HIGHLY EFFICIENT CATALYST FOR THE SYNTHESIS OF PYRANO[2,3-*d*]PYRIMIDINE DERIVATIVES IN AQUEOUS METHANOL MEDIA

D. S. Bhagat[a], M. V. Katariya[a], C. S. Patil[a], S. U. Deshmukh[a], S. U. Shisodia[a], S. S. Pandule[a] and R. P. Pawar[a]*

Keywords: Pyrano[2,3-*d*]pyrimidines; barbituric acid; aromatic aldehydes; Y$_2$O$_3$ catalyst.

Synthesis of pyrano[2,3-*d*]pyrimidine derivatives has been achieved by one-pot three component condensation reactions of various aromatic aldehydes, malononitrile and barbituric acid in aqueous methanol using yttrium oxide (Y$_2$O$_3$) as a catalyst. The potential application of Y$_2$O$_3$ in various synthesis increasing rapidly due to its reaction simplicity, minimum reaction time, high yields, environment friendly procedure and low cost of chemicals. The reactants are completely soluble in 70 % aqueous methanol and afford high yield of products.

* Corresponding Author
    Tel.: +91 0240 2334577; Fax: +91 0240 2334430.
    E-Mail: rppawar@yahoo.com
[a]   Department of Chemistry, Deogiri College, Station Road, Aurangabad 431 005, MS, India.

Introduction

Development of novel synthetic methodologies to facilitate the preparation of the desired molecule is an intense area of research. In this regard, efforts have been made constantly to introduce new methodologies that are efficient and more compatible with the environment.

Multicomponent reactions (MCRs) have received considerable attention of synthetic organic chemist from the last century due to the synthesis of different biologically active important complex heterocyclic molecules in single step. MCRs have emerged as efficient, atom economic, time saving and powerful tools in modern synthetic chemistry, as they increases the efficiency of the reaction along with saving time, solvents and chemicals.[1-3] The MCRs are combined with heterogeneous catalysts which can be recycled to give a green touch to these reactions.[4] Research in MCRs is an encouraging and hot topic of organic chemistry, because of their advantages in preparation of heterocyclic small molecule libraries and in drug discovery procedures.[5]

The pyrano[2,3-*d*]pyrimidine show biological activities as potential antiviral and antileishmanial,[6] anti-HIV,[7] antitubercular and antimicrobial,[8] antimicrobial,[9] antiplatelet,[10] antifungal,[11] antiviral,[12] bronchiodilator and vasodilator,[13] antiallergic,[14] antihypertensive and hepatoprotective,[15] antimalarial,[16] *invitro* antibacterial and antifungal agent.[17]

Several catalysts have been used for the synthesis of various 7-amino-5-phenyl-1*H*-pyrano[2,3-*d*]pyrimidine-2,4(3*H*, 5*H*)-dione derivatives such as DABCO,[18] NaBr,[19] L-Proline,[20] Triethylamine,[21] DAHP,[22] [KAl(SO$_4$)$_2$],[23] TBAF,[24] Piperidine,[25] [bmim]BF$_4$[26] and K$_2$CO$_3$.[27] Many of

the reported synthetic protocols are associated with the use of expensive reagents, extended reaction time, high reaction temperatures and tedious work-up procedures.

Herein we report the synthesis of pyrano[2,3-*d*]pyrimidine using recyclable and ecofriendly heterogenous catalyst yttrium oxide (Y$_2$O$_3$) by reacting aldehydes, malononitrile and barbituric acid in aqueous methanol (Scheme 1).
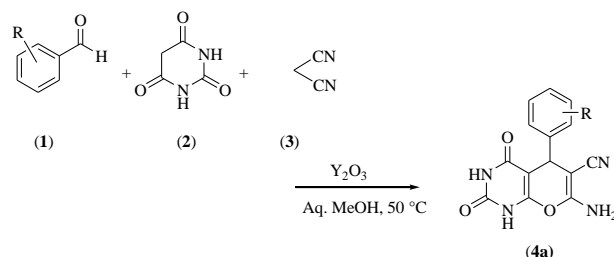
Scheme 1. Synthesis of pyrano[2,3-*d*]pyrimidine using Y$_2$O$_3$.

Experimental

All chemicals and reagents were purchased from commercial suppliers and used throughout without purification. Aromatic aldehydes, barbituric acid and malononitrile were purchased from Across organics. All solvents were purchased from Merck. Ethyl acetate, sodium sulphate and NaCl were purchased from Fisher Scientific.

The melting points of products are uncorrected. The ^{1}H NMR spectra was recorded on a Bruker Advance spectrometer operating at 400 MHz for ^{1}H at 295 K in CDCl$_3$. The chemical shifts were assigned in comparison with the residual proton and carbon resonance of the solvent DMSO (δ H=7.25 ppm) and TMS as the internal reference (δ=0 ppm). FTIR spectra were recorded on a Perkin-230 spectrometer in the range of 400-4000 cm^{-1} and peak positions are given as transmittance (%) against wave numbers (cm^{-1}).

General procedure for synthesis of 7-amino-5-phenyl-1H-pyrano[2,3-*d*]pyrimidine-2,4(3*H*,5*H*)-dione

In a round bottom flask, aromatic aldehyde (**1**) (1.00 mmol), barbituric acid (**2**), (1.00 mmol) and malononitrile (**3**) (1.00 mmol) and Y_2O_3 (10 mol %) in 70:30 MeOH:H_2O (2 mL) were taken and the reaction mixture was stirred at 50 °C. The progress of reaction was monitored by TLC using ethyl acetate-hexane (70:30) as a solvent system. The reaction mixture was quenched with crushed ice. The solid product was filtered, washed with ice cold water and recrystallized from ethanol to obtain pure pyrano[2,3-*d*] pyrimidine derivatives with excellent yields (90-96%).

7-Amino-2,3,4,5-tetrahydro-5-(4-nitrophenyl)-2,4-dioxo-1*H*-pyrano[2,3-*d*]pyrimidine-6-carbonitrile

IR (KBr): ν = 3441, 3352, 3189, 2982, 1726 cm⁻¹. ¹H NMR (400 MHz, DMSO-*d6*): δ = 10.87 (s, 1H, NH), 10.79 (s, 1H, NH), 6.98 (d, 2H, Ar-H), 6.82 (s, 2H, NH₂), 6.61 (d, 2H, Ar-H), 4.31 (s, 1H, CH) ppm.

7-Amino-5-(4-bromophenyl)-2,3,4,5-tetrahydro-2,4-dioxo-1*H*-pyrano[2,3-*d*]pyrimidine-6-carbonitrile

IR (KBr): ν = 3203, 3103, 2853, 1755, 1675, 1574 cm⁻¹. ¹H NMR (400 MHz, DMSO-*d6*): δ = 11.44 (s, 1H, NH), 11.30 (s, 1H, NH), 8.00-8.26 (m, 4H, Ar-H), 7.5-7.6 (s, 2H, NH₂), 3.31 (s, 1H, CH) ppm.

Results and Discussion

We have carried out reaction of an aromatic aldehyde, barbituric acid and malononitrile in the presence of yttrium oxide (Y_2O_3) as a catalyst in aqueous methanol (Scheme l). We varied several reaction parameters in order to optimize the reaction conditions, including an amount of the catalyst yttrium oxide, reaction temperature and use of different solvents. The best reaction conditions are when aromatic aldehyde (1.0 mmol), barbituric acid (1.0 mmol), malanonitrile (1.0 mmol) and Y_2O_3 (10 %) were reacted in 2 mL of 70:30 MeOH:H_2O for 30 min at 50 °C. Under these conditions 90-96 % of the product was achieved. In the absence of the catalyst, however, the only traces of product were obtained. To evaluate the exact concentration of yttrium oxide required for the optimum reaction, we have investigated the model reaction for the synthesis of compound (**4a**) using different concentrations of yttrium oxide, keeping the other conditions constant (Table 1).

Table 1. Optimization of the amount of catalyst Y_2O_3.

S. No.	Y_2O_3, mol %	Solvent	Yield, %
1	No catalyst	MeOH; H₂O	Traces
2	2	MeOH; H₂O	30
3	4	MeOH; H₂O	50
4	6	MeOH; H₂O	60
5	8	MeOH; H₂O	80
6	10	MeOH; H₂O	90
7	12	MeOH; H₂O	90
8	14	MeOH; H₂O	90

The results revealed that, when the reaction was carried out in presence of yttrium oxide up to 6 mol % of catalyst, it gave lower yield of product even after prolonged duration. Whereas optimum yields of product, were obtained by using 10 mol % of catalyst in shorter time, this concentration was ideal to carry out reaction smoothly. Further increasing in concentration of catalyst does not affect the yield of reaction (Table 1, entry 6, 7, 8). In order to evaluate the effect of different solvents, reactions were carried out in various solvents as enlisted in Table 2. Ethanol and DMSO resulted in good yields of 80% and 78%, respectively, whereas, aqueous methanol furnished the product in excellent yield of 90 % (Table 2, entry 6), making it the most suitable solvent.

Table 2. Influence of solvent on synthesis of pyrano[2,3-*d*]pyrimidines derivatives.

S. No.	Solvent	Yield, %
1	Toluene	60
2	Acetonitrile	70
3	DMF	75
4	DCM	70
5	Ethanol	80
6	Methanol (70%)	90
7	DMSO	78

Furthermore to study the reusability of the catalyst yttrium oxide (Y_2O_3), we have carried out model reaction of synthesis of 7-amino-5-(4-bromophenyl)-1*H*-pyrano[2,3-*d*]pyrimidine-2,4(3*H*, 5*H*)-dione by using 10 mol % of catalyst for up to 5 reruns. Recycling of the catalyst up to 3 runs show optimum results, after the 3rd run, it shows slightly decreased yield. The yields obtained by recycling of catalyst for the fresh run, 1st, 2ⁿᵈ, 3ʳᵈ, 4ᵗʰ and 5ᵗʰ reruns are, 92 %, 87 %, 85 %, 82 %, 78 % and 71 %, respectively.

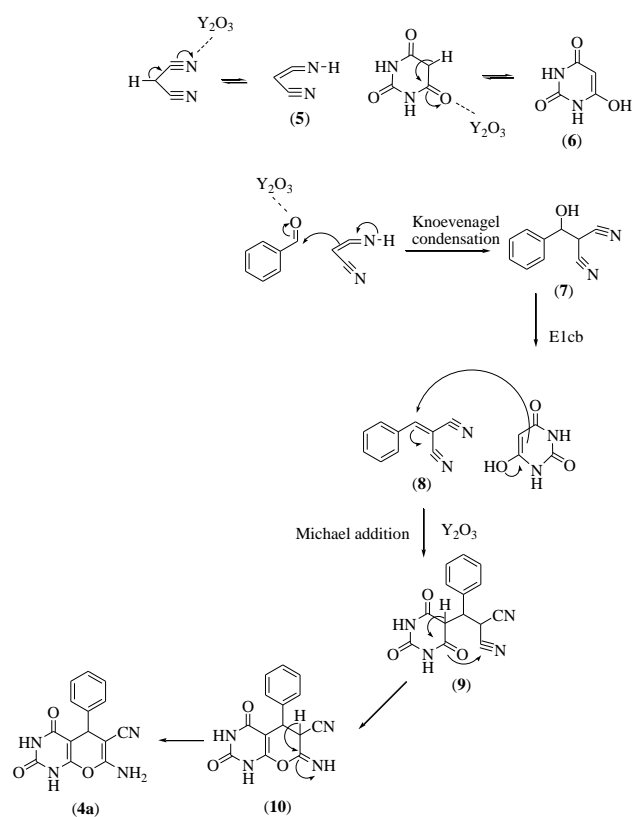**Table 3**. Synthesized pyrano[2,3-*d*]pyrimidines derivatives.

Compound	R	Time, min.	Yield, %	m.p., ⁰C
4a	H	30	90	204-206
4b	4-Nitro	30	92	248-250
4c	4-Bromo	35	95	220-222
4d	4-Hydroxy	30	92	228-230
4e	2-Chloro	30	95	240-242
4f	2,4-Dimethoxy	35	90	235-237
4g	2- Nitro	40	91	257-258
4h	3- Nitro	30	90	273-275
4i	3,4-Dimethoxy	35	91	303-306
4j	4-Methoxy	40	92	290-293
4k	4-Methyl	32	95	206-208
4l	4-Chloro	30	88	242-244
4m	3-Methyl	35	91	198-200
4n	3-Bromo	30	93	220-222
4o	2-Methoxy	38	88	230-232

To study the effect of structure of the aldehyde on the yield of the product pyrano[2,3-*d*]pyrimidines derivatives were synthesized by treating different aldehydes. Notably, all the substrates were observed to be well tolerated under optimized reaction conditions furnishing the product in good to excellent yields. Formation of the desired product was

confirmed by comparing their melting point and IR and ^{1}H NMR spectra with those of the reported compounds. The yields and m.p. etc. of the various pyrano[2,3-*d*]pyrimidines derivatives are given in Table 3.

Reaction mechanism

In the presence of yttrium oxide, malononitrile, and barbituric acid undergo enolisation to give (**5**) and (**6**), respectively. Yttrium oxide acts as a lewis acid catalyst.[28] in Knoevenagel condensation of the aromatic aldehyde and (**6**) to give intermediate (**7**), which on E[1]cb elimination gives intermediate (**8**). Michael addition reaction of (**6**) and (**8**) gives (**9**). The intermediate (**9**) on intramolecular cyclisation gives another intermediate (**10**), which on rearrangement gives the product pyrano[2,3-*d*]pyrimidine (**4a**).

Scheme 2. Plausible reaction mechanism for the synthesis pyrano[2,3-*d*]pyrimidines.

Conclusion

In present work, we have demonstrated the utility of the combination of yttrium oxide (Y$_2$O$_3$) and aqueous methanol for the synthesis of 7-amino-5-phenyl-1H-pyrano[2,3-*d*]pyrimidine-2,4(3*H*,5*H*)-dione from aromatic aldehydes, barbituric acid and malononitrile at room temperature. The presence of Lewis acidic sites (Y^{3+}) in the catalyst and aqueous methanol are good combination for the synthesis. It is sufficient enough to catalyze the reaction at ambient temperature affording (i) use of minimum reaction temperature, (ii) reduced reaction times, (iii) non-toxic and economically use of heterogeneous catalyst, (iv) eco-

friendly use of solvents, (v) high yield and (vi) easy separation are the significant advantages associated with the present protocol, which make it an attractive strategy for the synthesis 7-amino-5-phenyl-1*H*-pyrano[2,3-*d*]pyrimidine-2,4(3*H*,5*H*)-dione from aromatic aldehydes. This present protocol highlights and explores not only the applications of aqueous methanol as an excelent solvent in organic synthesis but also the reusability of Y$_2$O$_3$ as a good heterogeneous catalyst for the synthesis of heterocyclic compounds.

Acknowledgment

References

[1]Gore, R. P., Rajput, A. P., *Drug Invention Today*, **2013**, *5*, 148-152.

[2]Elders, N., Schmitz, R. F., Kanter, Ruijter, F. J. J., E., Groen, M. B., Orru, R. V. A., *J. Org. Chem.,* **2000**, *72*, 6135.

[3]Tekale, S. U., Pagore, V. P., Kauthale, S. S., Pawar R. P., *Chin. Chem. Lett.*, **2014**, *25*, 1149.

[4]Sharekh, S. *Res. J. Chem. Sci.,* **2014**, *4*, 18.

[5]Weber, L., *Drug Discovery Today,* **2002**, *7*, 143.

[6]Fan, X., Feng, D., Qua, Y., Zhang, X., Wang, J., Loiseau, P. M., Andrei, G., Snoeck, De Clercq, R., E., *Bioorg. Med. Chem. Lett.,* **2010**, *20*, 809.

[7]Magnus, M. A., Confalone, F. N., Storace, L., *Tetrahedron Lett.*, **2000**, *41*, 3015.

[8]Kamdar, N. R., Haveliwala, D. D., Mistry, P. T., Patel, S. K., *Eur. J. Med. Chem.* **2010**, *45*, 5056.

[9]Jain, S., Paliwal, P. K., Babu, A. G. N., Bhatewara, *J. Saudi Chem. Soc.,* **2014**, *18*, 535.

[10]Bruno, O., Brullo, C., Ranise, A., Schenone, S., Bondavalli, F., Barocelli, E., Ballabeni, V., Chiavarini, M., Tognolini, M., Impicciatore, M., *Bioorg. Med. Chem. Lett.,* **2001**, *11*, 1397.

[11](a) Akluwalia, V. K., Madhu, B., *Indian J. Chem.*, **1996**, *35*, 742. (b) Ahluwalia, V. K., Batla, R., Khurana, A., Kumar, R., *Indian. J. Chem.,* **1990**, *29*, 1141.

[12]Shamroukh, A. H., Zaki, M. E. A., Morsy, E. M. H., Abdel- F. M., Abdel-Megeid, F. M. E., *Arch. Pharm.,* **2007**, *340*, 236.

[13]Coates, W. J. *Eur. Pat.*, **1990**, *113*, 40711.

[14]Kitamura, N., Onishi, A., *Eur. Pat.,* **1984**, *104*, 186439.

[15]Furuya, S., Ohtaki, T., *Eur. Pat.,* **1994**, *121*, 205.

[16]Davoll, J., Clarke, J., Elslager, E. F., *J. Med. Chem.,* **1972.**

[17](a) Jayasree, J., *Ind. J. Engi. mat. Sci.*, **1997**, *4*, 232-236. (b) Ramalingam, S., Kumar, P., *Syn. Comm.*, **2009**, *39*, 1299.

[18]Bhat, R. A., Shalla, A. H., Dongre, R. S., *J. Adv. Res.,* **2014** (in press).

[19]Jain, S., Paliwal, P. K., Babu, G. N., Bhatewara, A., *J. Saudi Chem. Soc.,* **2014**, *18*, 535.

[20]Elinson, M. N., Ilovaisky, A. I., Merkulova, V. M., Zaimovskaya, T., Nikishin, G. I., *Mendeleev Commun.*, **2011**, *21*, 122.

[21]Bararjanian, M., Balalaie, S., Movassagh, B., Amani, A. M., *J. Iran. Chem. Soc*., **2009**, *6*, 436.

[22]Kostrub, V. V., Tsupak, E. B., Nelyubina, Y. V., *Mendeleev Commun.*, **2009**, *19*, 220.

[23]Balalaie, S., Abdolmohammadi, S., Bijanzadeh, H. R., Amani, A. M., *Mol Divers*, **2008**, *12*, 85.

[24]Bararjanian, M., Balalaie, S., Movassagh, B., Amani, A.M., *J. Iran. Chem. Soc.*, **2009**, *6*, 436.

[25]Kazemi-Rad, R., Kefayati, J. A. H., *Tetrahedron Lett.*, **2014**, *55*, 6887.

[26]Aly, H. M., Kamal, M. M., *Eur. J. Med. Chem.*, **2012**, *47*, 18.

[27]Fan, X., Feng, D., Qu Xinying, Y., Wang, Z. J., Loiseau. P. M., Andrei, G., Snoeck, R., De Clercq, E., *Bioorg. Med. Chem. Lett.,* **2010**, *20*, 809.

[28]Azzam, S. H. S., Pasha, M. A., *Tetrahedron Lett.*, **2012**, *53*, 7056.

GREEN SYNTHESIS OF STABLE SILVER NANOPARTICLES USING FLOWER EXTRACT OF *ROSA DAMASCENA*: CHARACTERIZATION, ANTIMICROBIAL AND ANTI-OXIDANT ACTIVITY STUDY

Mamatha Chekuri[a], Sindhu Gangarudraiah[a], Latha Bharadwaj Roopavatharam[a], Anubhav Kaphle[a] and Anupama Chalimeswamy[a]*

Biogenic synthesis of silver nanoparticles has attracted researcher's attention in recent days because of the necessity to develop new clean, cost effective and efficient techniques. In our study, we report green biogenic approach to synthesize silver nanoparticles using flower extract of *Rosa damascena* as reducing and stabilizing agent. The phytochemicals present in the petal extract induced the reduction of Ag^+ ions which resulted in the formation of conjugated nanoparticles. The formation and stability of the as-produced nanoparticles were monitored by UV-visible spectrophotometer that demonstrated an absorbance peak at around 412 nm corresponding to the plasmon resonance of silver nanoparticles. The average crystallite size of the particles calculated from the obtained XRD spectra using Debye Scherrer's formula was 4 nm. TEM results confirmed the formation of nano-sized polydispersed quasi-spherical shaped particles having the average diameter size of approximately 20 nm. Analysis of FTIR spectra revealed that the chemical moieties containing mainly amine, carboxyl, alcohol, esters functional groups coated the surface of the nanoparticles. Obtained nanoparticles were highly stable with no agglomeration even it is preserved for a period of 3 months and showed 'good' antibacterial activity.

* Corresponding Authors
    Mobile no: +91 9886027774
    E-Mail: canusri83@gmail.com, canusri@rediffmail.com
[a] Department of Biotechnology, Siddaganga Institute of Technology, Tumakuru 572 103, Karnataka, India.

Introduction

Nanotechnology has immense potential to provide solutions to technological and environmental challenges in the diverse area of molecular medicine,[1,2] bioremediation,[3,4] catalysis,[5,6] textile fabrics,[7,8] waste water treatment,[9-11] cosmetics.[12,13] Nanomaterials exhibit completely new or improved physicochemical properties due to their increased surface to volume ratio as well as the quantum confinement effects of size reduction, and thus have become an active area of research. Particularly, nanoparticles of noble metals such as silver have been explored tremendously due to their unique properties that can be easily tuned to confer them diverse utility.[14,15] For example, Optical property of silver nanoparticles known as surface plasmon resonance effects (SPR), which depends on the size and shape of the particles (and also on the dielectric of the medium[16] can be tuned to be used in various biomedical applications such as imaging or sensing.[17-19] Crystalline silver nanoparticles (SNPs) have also found significant applications in the field of high sensitivity biomarker detection and diagnostics[20] antimicrobials and therapeutics,[15,21] catalysis[22] and micro-electronics.[23,24] Silver nanoparticles were also prominent ingredients in Ayurvedic medical formulations; in the form of silver ash ('Ragatbhasma'), used to cure many major ailments. Moreover, because of the long established biocompatibility of silver nanoparticles, issues of any apparent nanotoxicity contributed by them within a dosage window will not be of a concern therefore making them sustainable for multiple uses.[25,26]

Different approaches such as reduction in solutions,[27] chemical reactions in reverse micelles,[28] gamma irradiation,[29] UV light irradiation,[30] microwave irradiation,[31] protecting electrolytic techniques by controlling electrode potential,[32] sonochemical,[33] and thermal decomposition of silver compounds[34] etc. have been used for the preparation of silver nanoparticles. However, these synthesis routes use hazardous chemicals, and/or extreme pressure and temperature conditions that are not very much desirable from the view of safety and economic viability. Also, trace amounts of unreacted precursor and aiding chemicals left behind as residues in the final product could pose potential harmful effects for end usages. Green synthesis approaches for the preparation of these kinds of nanomaterials can successfully eliminate toxic molecules involved in the synthesis process thereby making them more biocompatible. One green approach to synthesizing silver nanoparticles, also adapted in our study, is by using plant extracts that could avoid the use of synthetic stabilizing and capping agents as the plant materials can act alike.[35-37] Also, as compared to other biogenic approaches such as synthesis using microorganisms like bacteria[38,39] or fungi[40] plant mediated synthesis is more advantageous as it eliminates tedious processes of maintaining sterile cell cultures environment, and other biohazard issues related to them.

In our study, a simple approach to green synthesis of SNPs using flower extract of *Rosa demascena* as reducing and stabilizing agent has been assessed. *R. demascena* belongs to the plant family Rosaceae. It has received widespread attention due to its pharmacological properties that include anti-diabetic, anti-HIV and potential cure for cardiovascular diseases.[41,42] The petals of the flower have been reported to contain several important phytochemical groups, which include flavonoids, terpenes, anthocyanin, glycosides, carboxylic acid, vitamin C, myrcene, kaempferol and quercetin.[41] Therefore, in the view of the presence of

these many potent anti-oxidants and reducing agents[42] in the extract, we expected that it can be used for the rapid and efficient reduction of silver ions to silver nanoparticles.

The synthesis of the silver nanoparticles was optimized by taking several process parameters such as holding time, pH, temperature and concentration of precursors into account and going through one-factor-a-time approach to narrow down into optimized parameters. The obtained silver nanoparticles were then characterized, and the shape, size, morphology were assessed. The silver nanoparticles were also used to study their anti-microbial properties against bacterial species and fungal species namely *Escherichia coli, Pseudomonas aeruginosa, Staphylococcus aureus, Aspergillus niger* and *Fusarium solani* respectively.

Experimental

Sample collection and preparation of extract

Fresh flowers of *Rosa damascena* were purchased from the KR market, Bengaluru and were authenticated at the Department of Botany, Tumkur University, Tumakuru, India. The flowers were washed with de-ionised water before use to remove dirt and impurities on the petals.

Aqueous extracts of *Rosa damascena* flower petals were obtained using the following three methods. Fresh aqueous extraction without homogenization under boiling condition ('petal stripping'), homogenization of fresh petals followed by water extraction, and aqueous extraction from the dried flower powder under boiling. Among these approaches, fresh non-homogenized boiling method was adopted for our further studies because of the better extraction and quick reduction reaction observed based on the change in the solution color as well as the periodic UV test results.10 g of fresh flowers were washed for 4-5 times with deionized water and transferred to 250 ml of conical flask containing 100 ml of water and boiled with occasional stirring till the petals got decolorized, which took around 10-15 min. This solution was then cooled and filtered using Whatman No. 1 filter paper, and stored at 4° C for further use.

Phytochemical screening

Qualitative phytochemical screening was performed to obtain information about the presence of plant compounds such as saponins, alkaloids, flavanoids, tannins, proteins free amino acids, carbohydrates, vitamins and glycosides that may act as reducing and stabilizing agents. The protocol to perform the test was adapted from that of Bhandari et al.[43]

Biosynthesis of SNPs

1mmol of fresh AgNO$_3$ solution was prepared, its pH was adjusted to 10 using 1 % NaOH, kept on a magnetic stirrer and maintained at 60 °C. Fresh aqueous extract of *Rosa damascena* prepared by the 'petal stripping' method was added to the AgNO$_3$ solution drop wise. Change of the color of the solution from pale yellow to dark brown indicated the reduction of silver ions (Ag$^+$) into metallic silver nanoparticles, Ag(0). It took nearly one hour to complete the

reaction. The completion of the reaction was confirmed by periodic UV-vis spectra checks for the surface plasmon resonance (SPR) peak at around 420 nm. The final reaction solution was dialyzed against water using cellulose membrane of 12 KD cut-off value to remove unbound plant materials. The concentrated solution was then suspended in deionized water and centrifuged at 7000 rpm for 15 min. The process was repeated for 3-4 times to remove residual plant materials. The final solution was then stored, dried and the obtained powder was used for material characterization and application. We preserved some of our samples to check for the stability of particles.

Characterization

Silver nanoparticles were characterized using UV-visible spectroscopy, Fourier transfer infrared spectroscopy (FTIR), Transmission electron microscopy (TEM) and X-ray diffraction (XRD). UV-Visible spectroscopy was acquired with double beam spectrophotometer Schimadzu -1800. A quartz cell with a path length of 1 cm was used, and spectra were collected over a range of 200 -700 nm. XRD measurement of silver nanoparticles was carried out employing the Shimadzu-7000 X-ray diffractometer with monochromatized Cu Kα radiation operating at 40 KV and a current of 30 A at a scan rate of 0.388 min^{-1}. FTIR spectra were recorded using Agilent technologies Cary 630 FTIR. The scan was performed in the range of 800 to 4000 cm^{-1}. The morphology of silver nanoparticles were analyzed by using high resolution images obtained with FEI Techani G2 S-Twin TEM operating at 200 KV.

Antibacterial studies

The nanoparticles were tested for their antibacterial activity against two gram negative bacteria namely *Escherichia coli* (MTCC 1692) and *Pseudomonas aeruginosa* (MTCC 1688) and one gram positive bacteria *Staphylococcus aureus* (MTCC 3160) using standard well diffusion method.[44] Organisms were sub cultured on nutrient broths at 37 °C on a rotary shaker at 200 rpm until the absorbance reached around 0.4 to 0.6 at 600 nm to ensure that cells were in exponential phase. Muller Hilton agar media was prepared and poured into sterile Petri plates and allowed to solidify. The above sub cultured broths of respective organisms were swabbed on the solidified MH agar plates and allowed to dry for about 10 min. Wells of diameter size 6 mm were punched into the plates using a cork borer. 5 mg of the nanoparticle sample were suspended in 1 mL of deionized water and used as working concentration. Different aliquot sizes of 100 µL, 150 µL and 200 µL from the samples were added to corresponding well. Standard antibiotic Streptomycin was taken in a volume of 100 µL (5 mg/mL of final concentration) as the positive control. The plates were then incubated at 37 °C for 18-24 h for the development of inhibition zones. After the incubation time the zones of inhibition were observed and diameters of the zones were measured and tabulated.

Antifungal assay

The nanoparticles were tested for their antifungal activity against two fungal strains viz. *Aspergillus niger* (MTCC 4325) and *Fusarium solani* (MTCC 2027), using standard

well diffusion method. The pure cultures of the organism were sub cultured on potato dextrose broths at 37 °C on a rotary shaker at 160 rpm until spores were observed. Potato Dextrose Agar media was prepared and poured into sterile Petri plates and allowed it to solidify. The above prepared/sub cultured broth of respective organisms was swabbed on the solidified PDA plates and allowed to dry for about 10 min. The wells were punched on the plates using cork borer of diameter size 6 mm. 5 mg of sample was dissolved with 1 mL of deionized water and used as working concentration. Different volumes: 100 µL, 150 µL and 200 µL of the sample were added to each well. Standard Fluconazole powder was taken with volume of 100µL (5 mg/mL of final concentration) as positive control. The plates were then incubated at 28 °C for 2-4 days for development of inhibition zones.

Antioxidant assay

The anti-oxidant activity of the synthesized nanoparticles were evaluated using 2,2- diphenyl-1-picryl-hydrazyl radical (DPPH) radical scavenging assay which was originally described by Blois in 1958[45] and protocol for this assay was adopted from the work of Umesh et al.[46] The stock reagent solution was prepared by dissolving 24 mg of DPPH in 100 mL methanol and stored at -20 °C until use. The working standard solution was obtained by mixing 10 mL of stock solution with 45 m of methanol to obtain an absorbance value of ~1.1 at 517 nm. Aliquots of 50 µL, 100 µL, 150 µL and 200 µL of the nanoparticles were allowed to react with DPPH solution in the final reaction volume of 3 mL. 50 µL of methanol was made up to 3 mL by using DPPH solution. This was considered as negative control solut ion. The mixtures were shaken vigorously and allowed to stand in the dark condition at room temperature for about 30 min. The decrease in the absorbance of the resulting solution was then measured spectrophotometrically at 517 nm against methanol as blank. % of scavenging activity was calculated using the following formula,

$$\% RSC = 100 \times \left[1 - \frac{A_s}{A_c} \right]$$

where

% RSC depicts that free radical scavenging property of the sample,

A_s –absorbance of the sample,

A_c-absorbance of the control.

Results and discussion

Phytochemical screening

Preliminary qualitative phytochemical tests were performed on the extracts of *Rosa damascena* flowers prepared by all three methods of extraction as mentioned in the methodology part. All the extracts contained majority of group of secondary metabolite compounds namely saponins, alkaloids, flavonoids and tannins (phenolic compounds), carbohydrates, vitamin C and glycosides. Free amino acids

were absent in all the extracts. Proteins were present only in the extract obtained from fresh homogenization aqueous extraction. The absence of proteins in dried flowers extract may be due to the degradation of proteome over the drying period (Table 1).

Table 1. Phytochemical screening test.

S. No.	Phytochemical test	Method of extraction		
		Fresh petal strip extraction	Homogeni-zation	Dried flowers extraction
01	Saponins	+	+	+
02	Alkaloids	+	+	+
03	Flavonoids	+	+	+
04	Tannins	+	+	+
05	Proteins	-	+	-
06	Free amino acids	-	-	-
07	Carbohydrates	+	+	+
08	Vitamin C (ascorbic acid)	+	+	+
09	Glycosides	+	+	+

UV-Visible spectra

We did a series of experiments to optimize the production of silver nanoparticles with different concentration ratios of $AgNO_3$ and the extracts. Those samples were analyzed with the UV-visible spectroscopy. The rationale behind the optimization was; if any absorbance peak at around 420±10 nm was obtained from the synthesis solution for a given volume ratio of plant extract and silver nitrate solution, the ratio would be 'good' enough for the further synthesis process. It is showed the absorbance at 412 nm for the volume ratio of 1:0.5 corresponding to $AgNO_3$: extract ratio from 'Fresh petal stripping' extraction method. The 'Petal strip' method of extraction was selected for further synthesis because of the good stability and no agglomeration shown by the particles (Table 2).

Table 2. Optimization using different ratio of reactants.

S. No.	Aqueous extraction	$AgNO_3$:ex-tract ratio	Wavelength, nm
01	Fresh petal stripping	1:0.5	412
		8:2	409.50
02	Freshly homogenized	1:0.5	403.50
		8:2	408
03	Dried petal powder extraction	1:0.5	409
		8:2	410

Rosa damascena flower extract had an absorbance peak at around 270 nm and silver nitrate solution at 250 nm. After adding the extract to the silver nitrate solution, the solution turned to brown color and the wavelength shifted to around 412 nm (Figure 1) indicating the reduction reaction. And reaction was completed within 50 min.
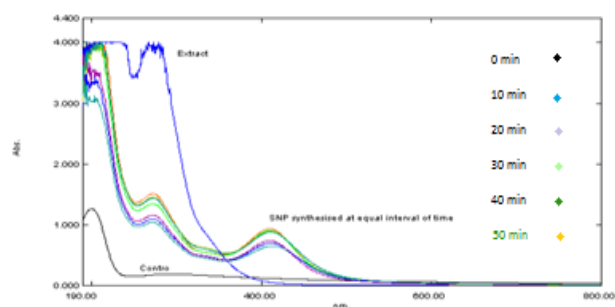
Figure 1. UV-Vis spectra of synthesized silver nanoparticles.

XRD studies

Nanocrystallinity of biosynthesized silver particles were confirmed using X-ray diffraction technique. The XRD pattern (Figure 2) showed numbers of Bragg reflections that may be indexed on the basis of the face-centered cubic structure of silver. It confirmed that the silver particles formed in our experiments were in the form of nanocrystals, as evidenced by the peaks at 2θ values of 38. 14 °, 44.46 °, 64.50 °, and 77.44 ° corresponding to (111), (200), (220), and (311) Bragg's planes respectively. The result indicates that synthesized nanoparticles were face centered cubic in structure (JCPDS file No. 84-0713 and 04-0783). The average cyrstallite size of our nanoparticles was calculated using the Debye-Scherrer equation, and corresponds to around 3.7 nm.
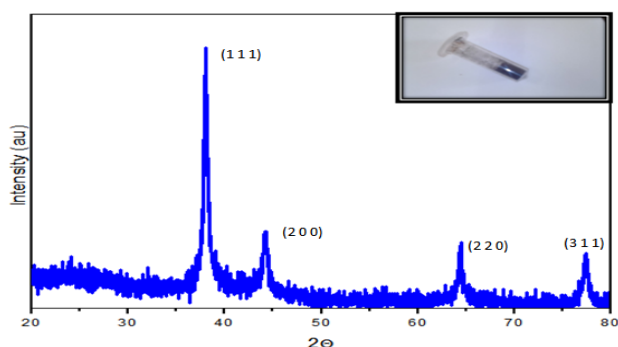

Figure 2. X-ray diffraction pattern for the synthesized silver nanoparticle.

TEM Analysis

The average actual particle size was measured using TEM. TEM images (Figure 3) confirm the formation of ultra-small sized silver nanoparticles. The particles are quasi-spherical in shape, poly-dispersed in nature and correspond to an average size of 20 nm.

FTIR spectra

FT-IR analysis was carried out to identify chemical groups localized on the surface of particles that could have been responsible for the reduction of silver salts into silver nanoparticles. Figure 4 shows the FTIR absorption spectra of the synthesized silver nanoparticles. The stretch in 2 or more bands, one stronger and broader than others occurring
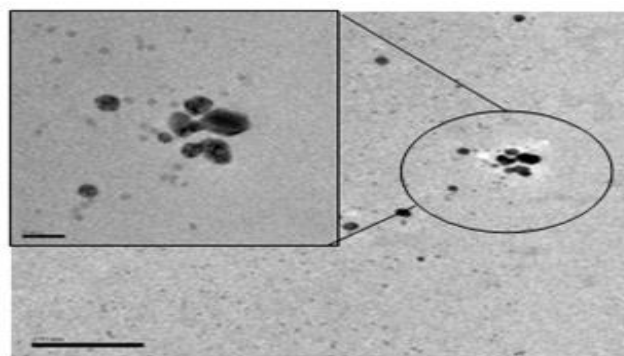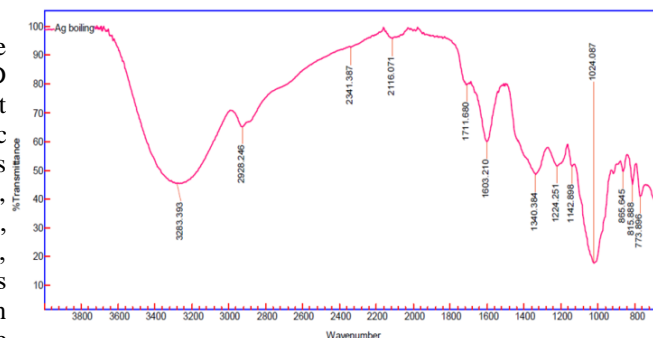

Figure 3. TEM image of prepared silver nanoparticles.

Figure 4. FTIR spectra for silver nanoparticles.

in the range of 1300-1000 cm^{-1} i.e., peaks centered at 1340, 1224, 1024, 1142 cm^{-1} are due to the stretching vibrations of C-O groups of anhydrides, esters, ethers, alcohols and phenols, C-O-H of alcohols and phenols, and of C-N of amines. The stretch observed at 1603 cm-^{1} may be due to the vibration of C=C group of alkenes, N-H of amides, and amine salts. The broad stretch occurring in the range of 3400-2400 cm^{-1}, which is centered at 3283 cm^{-1}, may well be due to stretching vibrations of N-H of amines, amine salts, sulfonamides, C-H of alkenes and alkanes, and C=O of carboxylic acids. The other weak bands observed in the graph indicate the presence of nitriles, aromatic rings and aldehydes. Thus, FTIR study indicates that –C=O (carboxyl), -OH (hydroxyl) and N-H (amine) groups in the flower extract were mainly involved in reduction of Ag+ ions to Ag^{0} nanoparticles. The FTIR spectroscopic study also suggest the role of carboxylic acid and ascorbic acid present in the flower extract as reducing and stabilizing agents for silver nanoparticles.

Biological activity assay

The antibacterial assay was carried out by employing standard well diffusion method against *E. coli, P.aeruginosa* and *S. aureus* and the inhibition zones are observed against standard of 5mg/ml streptomycin sulphate. The photographs in the Figure 5. As can be seen, *S. aureus* was most susceptible bacteria amongst the tested ones. As nanoparticles are showing little zone of inhibition against gram positive bacteria (S. aureus) compared to gram negative bacteria. After storing for 3 months also it does not showed any agglomeration and these nanoparticles are good enough to break the cell wall barrier of gram positive bacteria, even if it is thick.

Considerable inhibition zone for fungal samples were not observed in the assay.The antifungal activity of SNPs depends on the type of fungal species,size and shape of nanoparticles.[47]

Figure 5. Antibacterial assay plates for *S. auereus* (S.a), *P. aeruginosa(P.a)* and *E. Coli,* respectively.

We tested anti-oxidant scavanging activity of both the plant extract as well as the silver nanoparticles using DPPH assay. Silver nanoparticles showed less scavanging activity compared to the flower extract with % of scavanging of 22.17 for 150 µL of the silver nanoparticles suspension. For the same volume of sample, rose extract showed 81.1 % of scavanging activity This may be due to the oxidation of the anti-oxidant molecules from the extract during the reduction of silver ions so that they could not donate electrons to the free radicals. All results confirmed that silver nanoparticles are synthesized successfully without agglommeration. Even it is stored for few months   it is showing antibacterial activity against gram positive bacteria. Hence, by considering in view of cost effective production of silver nanoparticles by green method. It can be a promissing substitute route to use as a good antibacterial agent against multidrug resistant bacteria.

Conclusion

Silver nanoparticles with an average size of approximately 20 nm have been synthesized employing bio reduction method. Phytochemical screening of plant extract showed positive results for saponins, alkaloids, flavanoids, carbohydrates and glycosides. The synthesized silver nanoparticles were characterized by UV-vis spectrophotometry with absorbance wavelength at around 412 nm which is the suitable range for silver nanoparticles to exhibit surface Plasmon resonance. Multiple peak analysis of the XRD spectra confirmed the synthesis and indicated the crystallite size of our nanoparticles to be of ~4 nm. In addition, characterization done using FT-IR confirmed the presence of functional groups like alkanes, alkenes, alkynes, alcoholic and phenolic groups adhered on the surface of the particles. The conclusive evidence from phytochemical tests, UV-Visible spectroscopy and FT-IR revealed that the inherent action of reduction of silver nitrate to crystalline silver nanoparticles could be assigned to the compounds containing functional group C=O.

The prepared nanoparticles showed antibacterial effects with considerable inhibition in the growth of *S. aureus*. The particles did not show much effect on the fungal growth. *Rosa damascena* flower extract acts as a good reducing and stabilizing agent for the synthesis of silver nanoparticles in an eco-friendly and cost effective way. Particles were

observed to be highly stable for a period of 3 months. These biologically synthesized silver nanoparticles could be of immense use in medical field for their efficient antimicrobial function.

References

[1]Donner, A., *Trends Mol. Med.,* **2010**, *16*, 551-552.

[2]Roco, M. C., *Curr. Opin. Biotechnol.* **2003**, *14*, 337-346.

[3]Duran, N., *Rev. cienc. suelo. nutr. veg.,* **2008**, *8*, 33-38.

[4]Rajendran, P., Gunasekaran, P., *Environmental Bioremediation Technologies*, Springer **2007**, 211-221.

[5]Daniel, M.-C., Astruc, D., *Chem. Rev.,* **2004**, *104*, 293-346.

[6]Zhou, B., Hermans, S., Somorjai, G. A. *Nanotechnology in Catalysis,* Vol. 1, Springer, **2003.**

[7]Perelshtein, I., Applerot, G., Perkas, N., Guibert, G., Mikhailov, S., Gedanken, A., *Nanotechnology,* **2008**, *19*, 245705.

[8]Wang, R. R., Nasir, A., *Nanotechnology in Dermatology*, Springer, **2013,** 41-49.

[9] K Goyal, A., S Johal, E., Rath, G., *Curr. Nanosci.,* **2011**, *7(4)*, 640-654.

[10] Kanchi, S., *J. Environ. Anal. Chem.,* **2014**, *1*, e102.

[11]Theron, J., Walker, J., Cloete, T., *Crit. Rev.Mmicrobio.,* **2008**, *34*, 43-69.

[12] Katz, L. M., Dewan, K., Bronaugh, R. L., *Food Chem. Toxicol.*, **2015**.

[13]Kogure, K., Hama, S., *Nanomaterials for Cosmetics*, (2014).

[14]Shan, J., Tenhu, H., *Chem. Commun.,* **2007**, 4580-4598.

[15]Sondi, I., Salopek-Sondi, B., *J. Colloid Interface Sci.,* **2004**, *275*, 177-182.

[16]Miller, M. M., Lazarides, A. A., *J. Phys. Chem. B,* **2005**, *109*, 21556-21565.

[17]Jain, P. K., Huang, X., El-Sayed, I. H., El-Sayed, M. A., *Plasmonics,* **2007**, *2*, 107-118.

[18]Lee, K.-S., El-Sayed, M. A., *J. Phys. Chem. B,* **2006**, *110*, 19220-19225.

[19]McFarland, A. D., Van Duyne, R. P., *Nano lett.,* **2003**, *3*, 1057-1062.

[20]Minghui, Y., Jianxiu, W., Feimeng, Z., *Functional Nanoparticles for Bioanalysis, Nanomedicine, and Bioelectronic Devices Volume 1,* **2012**, *1112*, 177-205.

[21]Rai, M., Yadav, A., Gade, A., *Biotechnol. Adv.,* **2009**, *27*, 76-83.

[22]Xu, R., Wang, D., Zhang, J., Li, Y.,*Chem. Asian J.,* **2006**, *1*, 888-893.

[23]Gittins, D. I., Bethell, D., Schiffrin, D. J., Nichols, R. J., *Nature,* **2000**, *408*, 67-69.

[24]Lee, K. J., Jun, B. H., Choi, J., Lee, Y. I., Joung, J., & Oh, Y. S., *Nanotechnology,* **2007**, *18*, 335601.

[25]Lin, J.-J., Lin, W.-C., Li, S.-D., Lin, C.-Y., &Hsu, S.-h., *ACS Appl. Mater. Interfaces,* **2013**, *5*, 433-443.

[26]Pauksch, L., Hartmann, S., Rohnke, M., Szalay, G., Alt, V., Schnettler, R., Lips, K. S., *Acta biomate.,* **2014**, *10*, 439-449.

[27]López-Miranda, A., López-Valdivieso, A., Viramontes-Gamboa, G., *J. Nanopart. Res.,* **2012**, *14*, 1-11.

[28]Taleb, A., Petit, C., Pileni, M., *Chem. Mater.,* **1997**, *9*, 950-959.

[29]Soliman, Y., *Radiat. Phys. Chem.,* **2014**, *102*, 60-67.

[30]Huang, L., Zhai, M. L., Long, D. W., Peng, J., Xu, L., Wu, G. Z., Wei, G. S. *J. Nanopart. Res.,* **2008**, *10*, 1193-1202.

[31]Pal, A., Shah, S., Devi, S., *Mater. Chem. Phys.,* **2009**, *114*, 530-532.

[32]Rodriguez-Sanchez, L., Blanco, M., Lopez-Quintela, M., *J. Phys. Chem. B,* **2000**, *104*, 9683-9688.

[33]Jiang, L.-P., Wang, A.-N., Zhao, Y., Zhang, J.-R., Zhu, J.-J., Inorg. *Chem. Commun.,* **2004**, *7*, 506-509.

[34]Jeevanandam, P., Srikanth, C. K., Dixit, S., *Mater. Chem. Phys.,* **2010**, *122*, 402-407.

[35]Kotakadi, V. S., Gaddam. S. A.. Rao. Y. S., Prasad, T., Reddy, A. V., Gopal, D. S., *Eur. J. Med. Chem.,* **2014**, *73*, 135-140.

[36]Kotakadi, V. S., Rao, Y. S.. Gaddam. S. A., Prasad, T., Reddy, A. V., Gopal, D. S., *Colloids Surf., B: Biointerfaces,* **2013**, *105*, 194-198.

[37]Ponarulselvam, S., Panneerselvam, C.. Murugan, K., Aarthi, N., Kalimuthu, K., Thangamani, S., *Asian Pac. J. Trop. Biomed.,* **2012**, *2*, 574-580.

[38]Das, V. L., Thomas, R., Varghese, R. T., Soniya, E., Mathew, J., Radhakrishnan, E., *3 Biotech,* **2014**, *4*, 121-126.

[39]Deepak, V., Kalishwaralal, K., Pandian, S. R. K., Gurunathan, S., *Metal Nanoparticles in Microbiology,* Springer, **2011**, 17-35..

[40]Ahmad, A., Mukherjee, P., Senapati, S., Mandal, D., Khan, M. I., Kumar, R., Sastry, M., *Colloids Surf., B: Biointerfaces,* **2003**, *28*, 313-318.

[41]Boskabady, M. H., Shafei, M. N., Saberi, Z., Amini, S., *Iran J. Basic Med. Sci.,* **2011**, *14*, 295.

[42]Sagdiç, O., Baydar, N., & Baydar, H., *Food Sci. Technol. Int.,* **2004**, *10*, 277-281.

[43]Bhandary, S. K., Kumari, N., Bhat, V. S., Sharmila, K., & Bekal, M. P., *J. Health Sci.,* **2012**, *2*, 35-38.

[44]Palaksha, M., Ahmed, M., Das, S., *J. Nat. Sci. Biol. Med.,* **2010**, *1*(1), 12.

[45]Blois, M. S. , *Biochim. Biophys. Acta,* **1955**, *18*, 165

[46]Jagtap, U. B., Waghmare. S. R.. Lokhande, V. H., Suprasanna, P., Bapat, V. A., *Ind. Crop Prod.,* **2011**, *34*, 1595-1601.

[47]Medda. S.. Hajra, A., Dey, U., Bose, P., Mondal, N. K., *Appl. Nanosci.,* **2014**, 1-6.

A NEW REAGENT FOR THE SYNTHESIS OF PYRAZOLO[4,3-*e*][1,2,4]TRIAZOLO[1,5-*c*]PYRIMIDINES

Khidmet S. Shikhaliev[a], Evgeniya A. Kosheleva[a], Lyudmila F. Ponomaryeva[a], Michael Yu. Krysin[a]*

Tandem reaction of N'-(4-cyano-1-phenyl-1*H*-pyrazol-5-yl)-N,N-dimethylimidoformamide (**6**) with acylhydrazines in N,N-dimethylacetamide leads to the formation of 2-*R*-7-phenyl-7*H*-pyrazolo[4,3-*e*][1,2,4]triazolo[1,5-c]pyrimidines (**10a-f**).

* Corresponding Author
    Fax: +7 473 2208755
    E-Mail: kaf261@rambler.ru
[a]   Department of Chemistry, Voronezh State University, Universitetskaya pl. 1, Voronezh, 394006, Russian Federation

Introduction

The adenosine receptors ligands considered as prospective and promising candidates for treatment of diseases pathogenesis of which is connected with infringement the regulatory processes with involvement of adenosine (neurodegenerative, psychiatric, inflammatory disorders, diabetes, cancer, etc.). Derivatives of pyrazolo[4,3-*e*][1,2,4]triazolo[1,5-*c*]pyrimidines attract much attention among the nonpurine heterocyclic antagonists of that receptors, for which the affinity to three subtypes (A2A, A2B, A3) was revealed.[1-11] Also [11C] - and [18F] – radio-labeled pyrazolo[4,3-*e*][1,2,4]triazolo[1,5-*c*]pyrimidines have been developed as positron emission tomography tracers for the imaging of cerebral adenosine A2A receptors.[12,13]

A known synthetic approach to the heterocyclic system pyrazolo[4,3-*e*][1,2,4]triazolo[1,5-*c*]pyrimidine is sequential annelation of pyrimidine and triazole moieties to the pyrazole cycle (Scheme 1).[2-4,7,14,15]

The imidoformates (**2**), which were obtained by reaction of aminopyrazoles (**1**) with orthoethers R2C(OR1)3 (step i), give pyrazolo[3,4-*d*]pyrimidines (**3**) on interaction with hydrazines R3NHNH2 (step ii). An annelated triazole cycle formation takes place as a result of condensation of (**3**) with aromatic aldehydes (step iii, R3 = H, R4 = Ar).[15] The desired product can also be obtained by directly treating (**2**) with monoacylhydrazines. In such case intermediate (**3**) is usually are not isolated (step ii+iii, R3 = R4CO).[2-4,7,14] Despite the relative simplicity of the preparation of (**2**), this compound does not have thermal stability.

Moreover, fairly drastic conditions of heterocyclisation with acylhydrazides (high reaction temperature and long reaction time, on an average 10 h) and chromatographic purification of desired product are disadvantages of synthesis the method above.

It is, however, known that the corresponding dimethylaminomethylene(imido) derivatives are easily formed on the interaction of N,N-dimethylformamide dimethylacetal (DMFDMA, **5**) with compounds having substituents with labile hydrogen atoms (methyl, methylene, amino groups). These compounds eliminate dimethylamine on reacting with nucleophilic reagents resulting in a growth of carbon and heteroatom chain including in synthesis of heterocyclic compounds.[16]
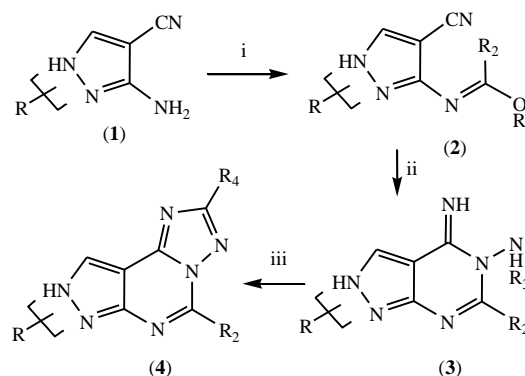
Scheme 1. Known synthetic route to pyrazolo[4,3-*e*][1,2,4]triazolo[1,5-*c*]pyrimidine scaffold.

The aim of the work is to investigate the possibility reacting *N'*-(4-cyano-1*H*-phenyl-1*H*-pyrazol-5-yl)-*N,N*-dimethylimidoformamide (**6**), a synthetic analog of imidoformates (**2**), with acylhydrazines in a one-pot synthesis of pyrazolo[4,3-*e*]1,2,4]triazolo[1,5-*c*]-pyrimidines.

Experimental

Instrumentation

^{1}H NMR spectra were recorded on the spectrometer Bruker DRX-500 (500.13 MHz) in ДМСО-*d6* as solvent and with TMS as an internal standard. Elemental analysis was performed on the elemental analyzer Perkin Elmer 2400. The melting points were determined on SMP-30.

The control reaction and compound purity were carried out by TLC on Merck TLC Silica gel 60 F$_{254}$ plates with UV - light 254 nm for visualization and CHCl$_3$, i-PrOH, or CHCl$_3$/EtOAc (5:1) as eluents.

Synthesis of N'-(4-cyano-1-phenyl-1H-pyrazol-3-yl)-N,N-dimethylimidoformamide (6).

A mixture of 1.84 g (10 mmol) 5-amino-4-cyano-1-phenylpyrazole (**1**) and 2.0 ml (1.78 g, 15 mmol) (**5**) in 1 ml *N,N*-dimethylacetamide (DMAA) was heated under reflux for 3 h. The residue, precipitated on cooling, was filtered and recrystallized from i-PrOH. The product was obtained as a beige powdery substance, yield 2.15 g (90 %). m.p. 94-95 °C. ^{1}H NMR δ: 2.97 (s, 3H, CH$_3$), 3.11 (s, 3H, CH$_3$), 7.33 -7.36 (m, 1H, Ph), 7.46-7.50 (m, 2H, Ph), 7.74-7.77 (m, 2H, Ph), 7.98 (s, 1H, Me$_2$NCH=N), 8.25 (s, 1H, pyrazole ring). Anal. calcd. for C$_{13}$H$_{13}$N$_5$: C, 65.25; H, 5.48; N, 29.27 %; Found: C, 65.31; H, 5.41; N, 29.34 %.

General procedure for the synthesis of 2-R-7-phenyl-7H-pyrazolo[4,3-e][1,2,4]triazolo[1,5-c]pyrimidines (10a-f)

The mixture of 10 mmol (**6**) and 10 mmol of the carboxylic acid hydrazide (**7**) were refluxed for 2-3 h in DMAA (5 ml). The precipitate, obtained on cooling, was filtered and recrystallized from mixture of i-PrOH-DMF (5:1). The resulted pyrazolotriazolopyrimidines (**10**) are white powdery substances.

2,7-Diphenyl-7H-pyrazolo[4,3-e][1,2,4]triazolo[1,5-c]pyrimidine (10a).

Yield = 76 %. m.p. 219-220 °C. ^{1}H NMR δ: 7.53-7.66 (m, 6H, benzene rings), 8.13-8.16 (m, 2H, benzene rings), 8.26-8.30 (m, 2H, benzene rings), 8.80 (s, 1H, pyrazole ring), 9.72 (s, 1H, pyrimidine ring). Anal. calcd. for C$_{18}$H$_{12}$N$_6$: C, 69.22; H, 26,91; N, 3,87 %; Found: C, 69.15; H, 26.86; N, 3.93 %.

2-(4-Methoxyphenyl)-7-phenyl-7H-pyrazolo[4,3-e][1,2,4]triazolo[1,5-c]pyrimidine (10b).

Yield = 72 %. m.p. 231 - 232 °C, (lit. 232 - 233 °C[14]). ^{1}H NMR δ: 3.85 (s, 3H, MeO), 7.13 (d, 2H, *J* = 8.7 Hz, p-MeOC$_6$H$_4$), 7.48 (t, 1H, *J* = 7.4 Hz, Ph), 7.62-7.65 (m, 2H, Ph), 8.15 (d, 2H, *J* = 8.0 Hz, Ph), 8.21 (d, 2H, *J* = 8.7 Hz, p-MeOC$_6$H$_4$), 8.80 (s, 1H, pyrazole ring), 9.70 (s, 1H, pyrimidine ring). Anal. calcd. for C$_{19}$H$_{14}$N$_6$O: C, 66.66; H, 24.55 ; N, 4.12 %; Found: C, 66.56; H, 24.51; N, 4.23 %.

2-(3-Chlorophenyl)-7-phenyl-7H-pyrazolo[4,3-e][1,2,4]triazole-[1,5-c]pyrimidine (10c).

Yield = 81 %. m.p. 246 - 247 °C. ^{1}H NMR δ: 7.49 (t, 2H, *J* = 7.3 Hz, benzene rings), 7.63-7.67 (m, 3H, benzene rings), 8.15 (d, 2H, *J* = 7.9 Hz, benzene rings), 8.22-8.25 (m, 2H, benzene rings), 8.85 (s, 1H, pyrazole ring), 9.78 (s, 1H, pyrimidine ring). Anal. calcd. for C$_{18}$H$_{11}$ClN$_6$: C, 62.34; H, 24.23; N, 3.20 %; Found: C, 62.24; H, 24.28 ; N, 3.25 %.

7-Phenyl-2-pyridin-4-yl-7H-pyrazolo[4,3-e][1,2,4]triazolo[1,5-c]pyrimidine (10d).

Yield = 67 %. m.p. 268 - 269 °C. ^{1}H NMR δ: 7.48-7.52 (m, 1H, benzene or pyridine ring), 7.66 (t, 2H, *J* = 7.9 Hz, benzene or pyridine ring), 8.15 (d, 2H, *J* = 7.9 Hz, benzene or pyridine ring), 8.19 (d, 2H, *J* = 5.9 Hz, benzene or pyridine ring), 8.83 (d, 2H, *J* = 5.9 Hz, benzene or pyridine ring), 8.88 (s, 1H, pyrazole ring), 9.84 (s, 1H, pyrimidine ring). Anal. calcd. for C$_{17}$H$_{11}$N$_7$: C, 65.17, H, 31.29, N, 3.54 %. Found: C, 65.22, H, 31.34, N, 3.48 %.

7-Phenyl-2-pyridin-3-yl-7H-pyrazolo[4,3-e][1,2,4]triazolo[1,5-c]pyrimidine (10e).

Yield = 78 %, m.p. 220-221 °C. ^{1}H NMR δ: 7.49-7.53 (m, 1H, benzene or pyridine ring), 7.64-7.66 (m, 2H, benzene or pyridine ring), 8.14-8.16 (m, 4H, benzene or pyridine ring), 8.60-8.62 (m, 1H, benzene or pyridine ring), 8.77-8.79 (m, 2H, benzene or pyridine ring), 8.88 (s, 1H, pyrazole ring), 9.82 (s, 1H, pyrimidine ring). Anal. calcd. for C$_{17}$H$_{11}$N$_7$: C 65.17, H 31.29, N 3.54 %. Found: C 65.23, H 31.37, N 3.45 %.

2-[(4-Chlorophenoxy)methyl]-7-phenyl-7H-pyrazolo[4,3-e]-[1,2,4]triazolo[1,5-c]pyrimidine (10f).

Yield = 77 %. m.p. 255-256 °C. ^{1}H NMR δ: 5.45 (s, 2H, CH$_2$), 7.13 (d, 2H, *J* = 9.0 Hz, p-ClC$_6$H$_4$), 7.37 (d, 2H, *J* = 9.0 Hz, p-ClC$_6$H$_4$), 7.48 (t, 1H, *J* = 7.4 Hz, Ph), 7.62-7.66 (m, 2H, Ph), 8.13 (d, 2H, *J* = 7.8 Hz, Ph), 8.79 (s, 1H, pyrazole ring), 9.73 (s, 1H, pyrimidine ring). Anal. calcd. for C$_{19}$H$_{13}$ClN$_6$O: C, 60.56; H, 22.30; N, 3.48 . Found: C, 60.62; H, 22.39; N, 3.35.

Table 1. Optimizing of reaction conditions of (**6**) with benzoic acid hydrazide (**7a**).

S.No	Solvent	Time, h	Results
1	Dioxane / TsOH (catalyst)	21	The reaction product is the resinous, chromato-graphically inseparable mixture
2	AcOH	16	The same
3	DMF	14	yield of 10a 52 %
4	DMAA	2.5	yield of 10a 76 %

Results and Discussion

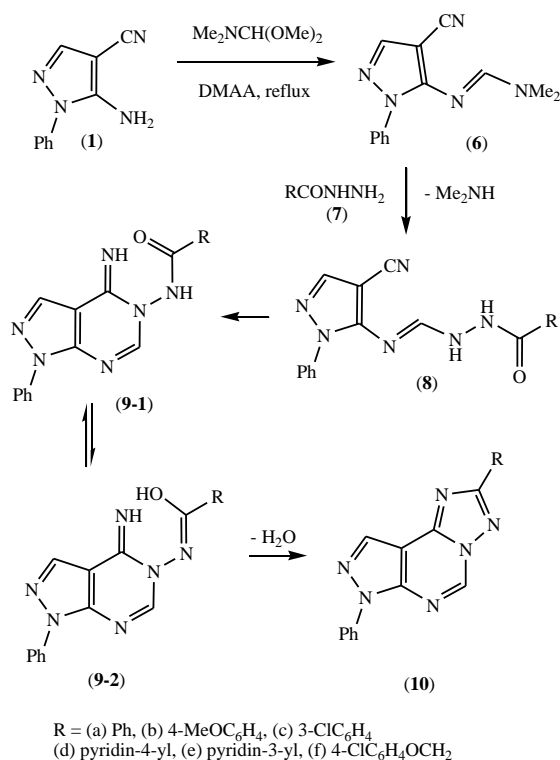*N'*-(4-Cyano-1-phenyl-1*H*-pyrazol-5-yl)-*N,N*-dimethylimidoformamide (**6**) was obtained from 5-amino-4-cyano-1-phenylpyrazole (**1**) and (**5**) according to a method that is similar to one proposed for 5-amino-4-cyano pyrazole with dimethylformamide diethylacetal. In this method there is no requirement for chromatographic purification.[17] This compound, unlike imidoformates (**2**), is stable during storage.

Optimization the reaction conditions of the reaction aromatic heterocyclic and aroxyacetic acids hydrazides (**7**) with (**6**) was carried out by an example of benzoic acid hydrazide (**7a**) (Table 1). The reactants were refluxed in the solvent for the time period mentioned in the table.

DMAA has found as optimal solvent. It provides comparable (or higher) yields of desired products in significantly shorter reaction time in comparison reported synthesis of (**2**).

In the ^{1}H NMR spectra of 2-*R*-7-phenyl-7*H*-pyrazolo[4,3-*e*][1,2,4]triazolo[1,5-*c*]pyrimidines (**10a-f**) there are two singlets near 8.8 and 9.7 ppm together with other protons signals of aryl and pyridine moieties (7.1-8.7 ppm), MeO-group (3.85 ppm, **10b**), methylene group (5.45 ppm, **10f**).The first singlet is corresponded to proton of pyrazole cycle (it is shifted to weaker field as compared to similar signal for starting compound (**6**), the second one corresponds to pyrimidine ring).

The interaction of (**6**) with acylhydrazides (**7**) is a tandem process (Scheme 2) that is similar to synthesis of pyrazolo[4,3-*e*][1,2,4]triazolo[1,5-*c*]pyrimidines from (**2**). In the first step there is an elimination of dimethylamine and formation of *N*'-[(4-cyano-1-phenyl-1*H*-pyrazol-5-yl)imino]methylhydrazide carboxylic acids (**8**), whose spontaneous heterocyclization leads to *N*'-(4-imino-1-phenyl-1,4-dihydro-5*H*-pyrazolo[3,4-*d*]pyrimidin-5-yl)ami-des (**9-1**). As a result of further cyclization, with water elimination, annelated triazolic cycle pyrazolo[4,3-*e*][1,2,4]triazolo[1,5-*c*]pyrimidines (**10**) is formed. Compound (**10**) can be also formed from N-substituted carboximidic acids (**9-2**) that are tautomeric forms of amides (**9-1**).

Conclusion

Thus, the interaction of *N*'-(4-cyano-1-phenyl-1*H*-pyrazol-5-yl)-*N*,*N*-dimethylimidoformamide (**6**) with carboxylic acid hydrazides in *N*,*N*-dimethylacetamide leading to 2-*R*-7-phenyl-7*H*-pyrazolo[4,3-*e*][1,2,4]triazolo[1,5-*c*]pyrimidines (**10a-f**) is a tandem process.

Acknowledgment

References

[1]Wilson, C. N., Mustafa, S. J., *Handbook of Experimental Pharmacology*, Springer Berlin, **2009**, 193.

[2]Gattal, F., Del Giudicel, M. R., Borionil, A., Borea, P. A., Dionisotti, S., Ongini, E., *Eur. J. Med. Chem.*, **1993**, *28*, 569.

[3]Baraldi, P. G., Cacciari, B., Romagnoli, R., Spalluto, G., Klotz, K.-N., Leung, E., Varani, K., Gessi, S., Merighi, S., Borea, P. A., *J. Med. Chem.,* **1999**, *42*, 4473.

[4]Baraldi, P. G., Cacciari, B., Romagnoli, R., Spalluto,G., Moro, S., Klotz, K. N., Leung, E., Varani, K., Gessi, S., Merighi, S., Borea, P. A., *J. Med. Chem.*, **2000**, *43*, 4768.

[5]Baraldi, P. G., Cacciari, B., Romagnoli, R., Spalluto,G., Varani, K., Gessi, S., Merighi, S., Borea, P. A.. *Drug Dev. Res.,* **2001***, 52*, 406.

[6]Pastorin, G., Da Ros, T., Spalluto, G., Deflorian, F., Moro, S., Cacciari, B., Baraldi, P. G., Gessi, S., Varani, K., Borea, P. A. *J. Med. Chem.*, **2003**, *46*, 4287.

[7]Okamura, T., Kurogi, Y., Hashimoto, K., Nishikawa, H., Nagao, Y. *Bioorg. Med. Chem. Lett.*, **2004**, *14*, 2443.

[8]Baraldi, P. G., Tabrizi, M.A., Romagnoli, R., Fruttarolo, F., Merighi, S., Varani, K., Gessi, S., Borea, P. A. *Curr. Med. Chem.*, **2005**, *12*, 1319.

[9]Pastorin, G., Da Ros, T., Bolcato, C., Montopoli, C., Moro, S., Cacciari, B., Baraldi, P. G., Varani, K., Borea, P.A., Spalluto, G. *J. Med. Chem.*, **2006**, *49*, 1720.

[10]Ortore, G., Martinelli, A. *Curr. Top. Med. Chem*., **2010**, *10*, 923.

[11]Baraldi, P. G., Saponaro, G. R., Romagnoli, R., Tabrizi, M. A., Baraldi, S., Moorman, A. R., Cosconati, S., Di Maro, S., Marinelli, L., Gessi, S., Merighi, S., Varani, K., Borea, P. A., Preti, D. *J. Med. Chem.*, **2012**, *55*, 5380.

[12]Moresco, R. M., Todde, S., Belloli, S., Simonelli, P., Panzacchi, A., Rigamonti, M., Galli-Kienle, M., Fazio, F. *Eur. J. Nucl. Med. Mol.,* **2005**, *32*, 405.

[13]Khanapur, S., Paul, S., Shah, A., Vatakuti, S., Koole, M. J. B., Zijlma, R., Dierckx, R. A. J. O., Luurtsema, G., Garg, P., van Waarde, A., Elsinga, P. H. *J. Med. Chem.*, **2014**, *57*, 6765.

[14]Tyurin, R. V., Vorob'ev, E. V., Minyaeva, L. G., Krasnikov, V. V., Mezheritskii V. V., *Russ. J. Org. Chem.*, **2005**, *41*, 916.

[15]Dolzhenko, A. V., Pastorin, G., Dolzhenko, A. V., Chui, W. K., *Tetrahedron Lett.,* **2009**, *50*, 5617.

[16]Abu-Shanab, F. A., Sherif, S. M., Mousa, S. A. S., *J. Heterocyclic Chem.*, **2009**, *46*, 801.

[17]Bulychev, Yu. N., Korbukh, I. A., Preobrazhenskaya, M. N., Chernyshov, A. I., Esipov, S. E., *Chem. Heterocycl. Comp.*, **1984**, *20*, 215.

R = (a) Ph, (b) 4-MeOC$_6$H$_4$, (c) 3-ClC$_6$H$_4$
(d) pyridin-4-yl, (e) pyridin-3-yl, (f) 4-ClC$_6$H$_4$OCH$_2$

Scheme 2. Plausible route of the formation of (**10**).

EVALUATION OF THE CHEMICAL AND MICROBIOLOGICAL CONTAMINATION OF THE RIVER SITNICA WATERS (KOSOVO): A STATISTICAL APPROACH

Fatbardh Gashi[a], Bardha Korca[a]*, Kemajl Kurteshi[b], Fatmir Faiku[a], Muhamet Domuzeti[a] and Sadije Gashi[a]

Chemical and microbiological contamination of ground water has several implications for human health. The study of chemical and microbiological contamination of water is carried out in Sitnica river (Kosova). Water samples are collected at 10 sampling points and fourteen different parameters are investigated. The program, Statistica 6.0, is used for calculations of basic statistical parameters and anomalies (extremes and outliers). The chemometric approach and the results yielded useful information about water quality and can lead to better water resource management. Dendograms and box-whisker plots are drawn to evaluate the chemical variation. The level of some microbiological and phsico-chemical parameters and eco-toxic ions from surface water are compared with the results from the river source where anthropogenic effects are negative. Our results show that chemical and microbiological pollutions are the results of anthropogenic factors coming from settlements, peripheral rivers and agricultural in the region surround.

* Corresponding Authors
    E-Mail: bardhakorca@gmail.com
[a]   Department of Chemistry, Faculty of Natural Sciences, St. M. Teresa 10, University of Prishtina, Kosovo
[b]   Department of Biology, Faculty of Natural Sciences, St. M. Teresa 10, University of Prishtina, Kosovo

Introduction

The sources of microbial and chemical contamination are numerous and include the land disposal of sewage effluents, sludge and solid waste, septic tank effluent, urban runoff, and agricultural, mining and industrial practices.[1,2] Chemical contamination of drinking water is often considered a lower priority than microbial contamination by regulators, because adverse health effects from chemical contaminations are generally associated with long-term exposures, whereas the effects from microbial contamination are usually immediate.[3] The quality of drinking water is an issue of primary interest for the residents of the European Union.[4] In peat bogs, water flows freely in the active layer of water or acrotelm. Water storage is critical to the balance of water in peat swamps and at surrounding areas. Logging activity, agriculture, peat extraction and destruction of peat swamp drainage activity also give a negative effect and has a bad implication on the hydrology.[5]

Decomposition of organic matter and pollution due to anthropogenic activity are the main sources of pollution of water.[6] Therefore, multidisciplinary collaborative research is essential for understanding the pollution processes. As reported by Brils,[7] adequate water quality in Europe is one of the most eminent concerns for the future. Good management of natural and environmental waters will give results if leading institutions constantly monitor information about environmental situation. Therefore, seeing it as a challenge for environmental chemists, our goal is to determine the amount and nature of pollutants in the environment.

This work is a continuation of our earlier studies of surface waters in Kosovo.[8-11] One could claim that the most polluted areas in the world are those with the dense population. It should therefore be the foremost goal of environmentalists to prevent such pollution, and to educate the population towards proper management of ecosystems.[12]

The aim of the current work is to perform, a systematic research on the water of Sitnica river. The research is about chemical and microbiological aspects as they affect directly and indirectly the water quality, also impact the aquatic life. A major impact will be on biota where a large amount of this river flow is used for irrigation of agricultural lands and thus it may have an indirect impact on people's lives as they consume agricultural products that can deposit pollutants in the body of people through the food chain.[13]

Experimental

Study area

The objective of this study is microbial and chemical examination of water quality of Sitnica (length = 90 km). Sampling strategy was planned at 10 monitoring stations spread over the source in the mountain and downstream to the end of the river within Kosovo's territory. Although there are more than 50 water quality parameters available, only 14 parameters are selected for our investigation. These parameters are: water temperature, conductivity, pH, turbidity, consumption of $KMnO_4$, total oxygen, nitrate nitrogen, nitrite nitrogen, ammonia nitrogen, total coliform, coliform bacteria of faecal origin, aerobic bacteria, sulfide-reducing anaerobic sporogens bacteria and streptococcus of faecal origin. The sampling sites are geographically positioned using geographic information system (GIS). The results are interpreted using modern statistical methods that can be used to

locate pollution sources. Surface water sampling of champions and their elaboration at the depth ≥ 20 cm are done with Pyrex non-contaminating bottles according to standards methods for surface water.[14] Some of the natural water samples are filtered with Whatman paper (0.45 μm) made from cellulose nitrate in the bottle of Teflon under pressure of nitrogen (purity 99.99 %).

Sampling and sample preparation

For chemical analysis water samples are collected on 3 March 2010 in plastic bottles, previously rinsed three times with sampled water, and labeled with the date and the name of the sample. These samples are transferred to refrigerator (at 4 °C) for analysis in the laboratories.

For bacteriological evaluation, samples, taken on 7 March 2010, in plastic sterile bottles are refrigerated (at 4°C) and transported immediately to laboratory and analyzed on the same day.

All tests are performed at least thrice to calculate the average value. The sampling locations are chosen at points where pollution is expected due to closeness of factories, traffic, settlements or combinations of these factors. Sampling, preservation and experimental procedure for the water samples are carried out according to the standard methods for examination of water.[15-18] Samples are preserved in refrigerator after treatment. The study area and the sampling locations are shown in Figure 1. The details about sampling sites are presented in Table 1.
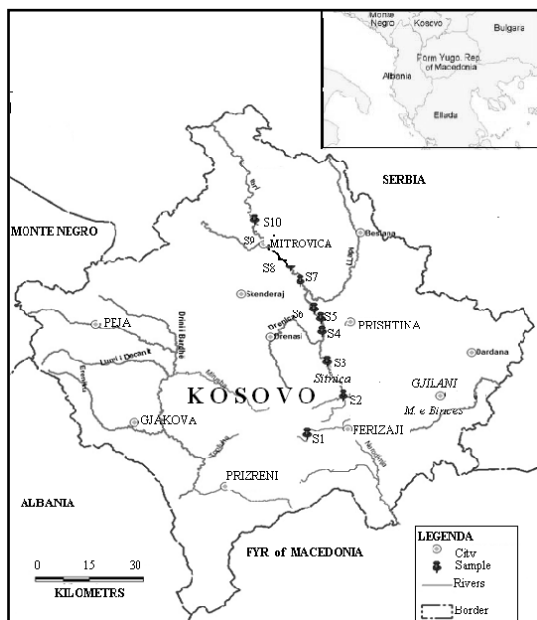

Figure 1. Study area with sampling stations.

Chemical and microbiological characterization

Double distilled water was used in all experiments. All instruments are calibrated according to manufacturer's recommendations. Temperature of water was measured immediately after sampling, using digital thermometer, model Quick 63142. pH measurements were performed using pH/ion-meter of Hanna Instruments. Electric conductivity is measured by InoLab WTW conductometer, turbidity with turbidimetric method with formazine standard, chemical expense with $KMnO_4$ using Thiemann Küebel volumetric method (boiling in acidic environment). Some of physico-chemical parameters (total oxygen, NO_2^-, NO_3^- and NH_4^+) are determined using UV-VIS spectrometry method.

Table 1. Detailed description of sampling stations.

Sample	Locality	Coordinates	Possible pollution sources
S$_1$	Jezerc	34T 0501340 UTH4689442	Settlement
S$_2$	Rubofc	34T 0511168 UTH0701529	Waste water, agriculture
S$_3$	Lypjan	34T 0509360 UTH4706698	Road, waste water from Lypjan
S$_4$	Lismir	34T 0505443 UTH4721072	Settlement, agriculture, flotation waste, waste water from Prishtina
S$_5$	Palaj	34T 0504992 UTH4725302	Agriculture, waste water from Fushë kosova
S$_6$	Plemetin	34T 0503152 UTH4728263	Thermal power plant, waste water from Kastriot
S$_7$	Pestova	34T 0499284 UTH4736665	Agriculture
S$_8$	Vushtrri (exit)	34T 0496273 UTH4741288	Agriculture, tin factory, waste water from Vushtrria
S$_9$	Mitrovica (exit)	34T 0490408 UTH4749416	Phosphate and accu factory, settlement, road, waste water from Mitrovica
S$_{10}$	Zveqan	34T 0487012 UTH4754445	Road, waste water from Mitrovica

The total coliform bacteria are evaluated at 30 °C (agar plate) according to probable number technique (MPN) per 100 mL. The coliform bacteria of fecal origin were evaluated at 44 °C (endo agar plate). The total aerobic bacteria in 1 mL are evaluated at 37 °C (plate count agar) according to "colony star" (Frank Gerber), 1MPN technique. Sulphide reducing anaerobic sporogens bacteria are evaluated at 37 °C (sulphite agar plate). The streptococcus bacteria of fecal origin are evaluated in 100 mL of water.

Statistical Methods

Program Statistica 6.0[19] is used for all statistical calculations such as determination of basic statistical parameters (mean, geometric mean, median, maximum minimum variance and standard deviations) and determination of anomalies (extremes and outliers) for solution data. Outlier values are between 1.5 and 3, and extreme values are above 3 standard deviations.

Results

The physico-chemical parameters i.e. water temperature, EC, pH, turbidity, consumption of $KMnO_4$, total oxygeny and concentrations of NO_2^-, NO_3^- and NH_4^+ are presented in Table 2.

Table 2. Some physico-chemical parameters of the river water

Sample	Water temp. /^{o} C	EC /μS cm^{-1}	pH /1	Turbidi-ty, / NTU	Cons. of MnO$_4^-$ /mg L^{-1}	TO /mg L^{-1}	NO$_2^-$ /mg L^{-1}	NO$_3^-$ /mg L^{-1}	NH$_4^+$ /mg L^{-1}
S$_1$	11.90	405	7.18	0.13	11.06	9.4	0.005	0.05	0.06
S$_2$	11.90	297	7.34	94	37.83	8.3	0.06	0.50	0.09
S$_3$	11.80	309	7.39	79	28.44	7.8	0.05	0.50	0.08
S$_4$	11.90	594	7.09	51	37.6	7.1	0.11	0.50	0.17
S$_5$	11.80	423	7.93	91	26.86	7.7	0.05	0.50	0.38
S$_6$	11.90	446	7.84	92	23.70	7.8	0.04	1.20	0.50
S$_7$	11.90	435	7.51	61	24.65	7.8	0.04	1.40	0.27
S$_8$	11.90	455	7.73	69	24.33	8.0	0.04	0.50	0.22
S$_9$	12.00	462	7.68	59	30.02	7.3	0.04	0.50	0.28
S$_{10}$	11.90	445	7.68	59	22.12	8.1	0.04	0.50	0.23

Table 3. Microbiological parameters of the river water

Sample	Coliform bacteria /100 mL	Coliform bacteria (faecal origin) /100 mL	Aerobic bacteria at 37 ^{0}C / 1 mL	Anaerobic sporogens sulphide reducing bacteria /100 mL	Streptococcus (faecal origin) /100 mL
WHO/MPN	100	0	300	10	0
S$_1$	0	0	0	0	0
S$_2$	>300	>300	>300	5	>300
S$_3$	300	300	>300	20	>300
S$_4$	>300	300	>300	10	300
S$_5$	>300	>300	>300	>20	>300
S$_6$	>300	>300	>300	>25	>300
S$_7$	>300	>300	>300	>100	>300
S$_8$	>300	>300	>300	>100	>300
S$_9$	>300	>300	>300	>50.0	>300
S$_{10}$	>300	>300	>300	10	>300

The bacteriological parameters viz. total coliform bacteria, coliform bacteria of fecal origin, number of aerobic bacteria, numbers of anaerobic sulphide reducing sporogens and streptococcus of fecal origin are presented in Table 3. The basic statistics of the measured data set and anomalous values (outliers and extremes) from 9 variables of water are summarized in Table 4. Using experimental data (Table 2) and box plot approach of Tukey[20], anomalous values (extremes and outliers) in waters were determined for the whole region (Figure 2).

Discussion

The temperature variation at different locations of the river, indicated by the in situ readings, is given Table 2. The pH of the investigated samples, ranging from 7.09 to 7.93, indicates that all water samples are slightly alkaline. Electrical conductivity, ranging from 297-594 μScm^{-1}, is within highest desirable limit (HDL). If we compare EC separately, the lowest value is observed at S$_2$ station and the highest value is observed at S$_4$ station. Higher EC values indicate the presence of higher content of dissolved salts in the water. The lowest value of turbidity is observed at point S$_1$ (near the river source) while at all points we observed higher values of turbidity coming

from settlements, gravel separations and anthropogenic waste. Consumption of KMnO$_4$ has maximum values at S$_2$ and S$_4$ while the lowest vale is at S$_1$. The total oxygen (TO) is in the range of 7.1 mg L^{-1} at S$_4$ and 9.4 mg L^{-1} at S$_1$(source of the river).

Presence of nutrient salt of nitrogen in water as ammonia, nitrites and nitrates causes the process of eutrophication.[21] The concentration of ammonia presents the potential risk for the aquatic organisms. Total ammonia values changed downstream of the river and the lowest value is found at point S$_1$ and highest value at points S$_5$ and S$_6$. The highest value of NO$_2^-$ is found at S$_4$ and that for NO$_3^-$ it is found at points S$_6$ and S$_7$. Concentration of NO$_2^-$, NO$_3^-$ and NH$_4^+$ are within highest desirable limit (HDL) according to WHO standards for drinking water.

Statistical methods are applied to find anomalous values also. Outlier value for NH$_4^+$ (0.5 μg L^{-1}) is found in the S$_5$ sample, extreme for NO$_2^-$ (0.11 μg L^{-1}) is in the S$_2$ sample and extreme for NO$_3^-$ (1.2-1.4 μg L^{-1}) is found in S$_6$ and S$_7$ samples.

The National Primary Drinking Water Regulations (NPDWRs) have prescribed limits of the amount of total coliforms, faecal coliform, *E. coli*, *Salmonella spp*.

Table 4. Basic statistical parameters for 9 variables in 10 water samples.

Variable	Descriptive Statistics						
	Mean	**Geo. mean**	**Median**	**Minimum**	**Maximum**	**Variance**	**SD**
Water temp. /°C	11.9	11.9	11.9	11.8	12.0	0.003	0.05676
EC /μS cm^{-1}	427.1	419.7	440.0	297.0	594.0	6885.656	82.97985
pH /1	7.54	7.53	7.56	7.09	7.93	0.079	0.28143
Turbidity/NTU	65.51	37.85	65.0	0.13	94.00	771.943	27.78386
Cons. of MnO$_4^-$ /mg L^{-1}	26.66	25.44	25.76	11.06	37.83	60.128	7.75423
TO /mg L^{-1}	7.93	7.91	7.80	7.10	9.40	0.391	0.62548
NO$_2^-$ /mg L^{-1}	0.0475	0.0391	0.0400	0.0050	0.1100	0.001	0.02617
NO$_3^-$ /mg L^{-1}	0.6150	0.4805	0.5000	0.0500	1.4000	0.152	0.39019
NH$_4^+$ /mg L^{-1}	0.2280	0.1874	0.2250	0.0600	0.5000	0.019	0.13911
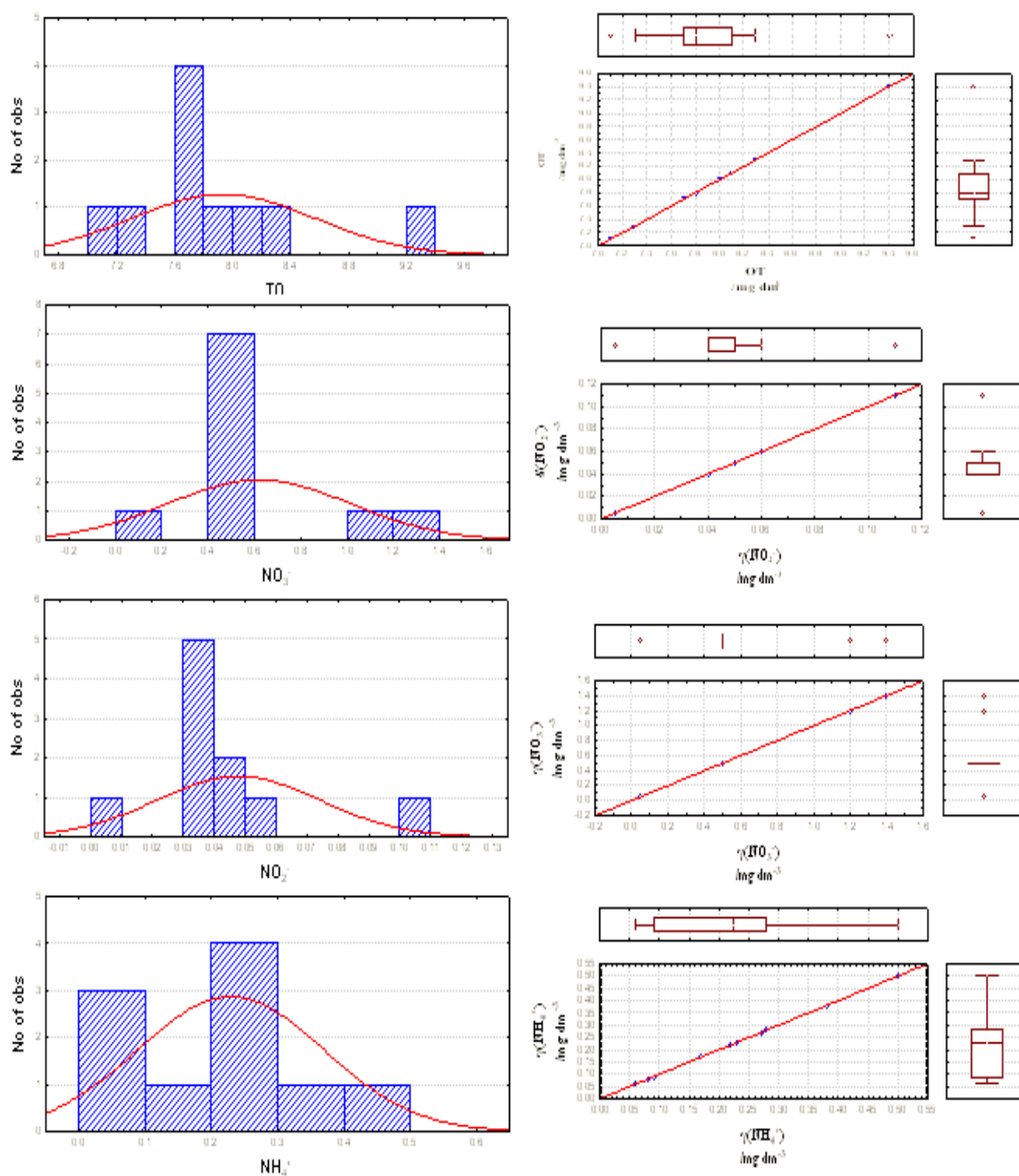
Figure 2. Frequency histograms and scatter box plot diagrams of 4 measured variables.

Shigella spp. and *Vibrio spp*. as primary standards to protect the health of the public by limiting the levels of contaminants in drinking water.[22] In the present study (Table 3) the number of total coliform bacteria in 100 mL river water is found to be greater than 300 in samples S_2-S_{10} and are well above recommended number by WHO standards (MPN = 100). The number of total coliform bacteria of faecal origin (in100 mL river water) is greater than 300 in samples S_2-S_{10} and are above recommended number by WHO standards (MPN = 0). Osuinde and Enuezie reported that high coliform count obtained in water samples may be attributed to faecal contamination of the water sources.[23] Hence none of the water samples analyzed complies with EPA standard for coliform in water. According to EPA standard, every water sample that has coliform must be analyzed for either faecal coliforms or *E. coli* to ascertain whether the source of contamination is from human or animal waste, and possibly pathogenic bacteria or organism, such as *Gardia* and *Cryptosporidium*, may be present. The number of aerobic bacteria in 1 mL at 37 °C are found to be greater than 300 in samples S_2-S_{10} (MPN = 300). The number of sulfide reducing anaerobic sporogens bacteria in 100 mL is above the recommended number by WHO standards (MPN = 10) in S_3 and in S_5-S_9. The number of streptococci bacteria of faecal origin in 100 mL is greater than 300 in samples S_2-S_{10} and therefore much above the recommended number by WHO standards (MPN = 0).

Conclusions

The chemical and microbiological analysis shows that Sitnica river water is highly polluted. Therefore this water cannot be used without previous physical and chemical treatment. A long and uncontrolled discharge of municipal waste impacts the water quality. The large number of total coliforms and coliforms bacteria in faecal origin, sulfide reducing bacteria and streptococcus bacteria, and high concentration of nutrient salt of nitrogen as ammonia, nitrites and nitrates showed the faecal contamination of the river Sitnica water in some samples is beginning to reach the aquifer. For this reason, we recommend avoiding the discharge of waste water without treatment, mainly from septic tanks, which are extensively used in the area.

Acknowledgements

References

[1]Close, M., Dann, R., Ball, A, Pirie, R., Savill, M. and Smith, Z., *New Zealan. J. Water Health.*, **2008**, *6(1),* 83–98.

[2]Keswick, B. H., *Groundwater Pollution Microbiology. New York: John Wiley and Sons.* **1984,** 39-64.**.**

[3]Thompson, T., Fawell, J., Kunikane, S., Jackson, D., Appleyard, S., Callan, P., Bartram, J. and Kingston, P., *Chemical safety of drinking-water: Assessing priorities for risk management, World Health Organization,* **2007.**

[4]Chirila, E., Bari, T., and Barbes, L., *Ovidius Univ. Ann. Chem.*, **2010,** *21,* 87-90.

[5]Hamilton, L. S., *1st Edition, Food and Agriculture Organization of the United Nation, Rome*, **2008**, 78.

[6]Montgomery, J. M., *Water Treatment, Principles and Design*. John *Wiley & Sons, New York,* **1996,** 474.

[7]Brils, J., *Ann. Inst. Superiore Sanita*. **2008**, *44,* 218–223.

[8]Gashi, F., Frančišković-Bilinski, S., Bilinski, H., Troni, N., Bacaj, M. and Jusufi, F., *Environ. Monit. Assess.,* **2011**, *75,* 279–289.

[9]Gashi, F., Faiku, F., Haziri, A., Hoti, R., Isufi, F., Laha, F., Shala, B., Feka, F., Dreshaj, A., *J. Int. Environ. Appl. Sci.*, **2012**, *2(3),* 530-537.

[10]Gashi, F., Faiku, F., Haziri, A., Hoti, R., Laha, F., Isufi, F., Rexhepi, A., Shala, M. and Hasanaj, A., *J. Int. Environ. Appl. Sci.,* **2012**, *7(2),* 373-380.

[11]Gashi, F., Troni, N., Faiku, F., Laha, F., Haziri, A., Kastrati, I., Beshtica, E. and Behrami, M., *Am. J. Environ. Sci.,* **2013**, *9(2),* 142-155.

[12]Šajn, R., Bidovec, M., Andjelov, M., Piric, S. and Gosar, M., *Geochemical atlas of Ljubljana and surround. Geološki Zavod Slovenije (Geological Survey of Slovenia),* Ljubljana, **1998,** 670,

[13]Pecsok, R. and Shields, L. *Modern Methodes of Chemical Analysis*, *John Wiley & Sons. Inc., New York, London, Sidney.* **1968.**

[14]Hurd, D. C., Spencer, D. W., *American Geophysical Union, Geophysical Monograph.,* **1991,** 63.

[15]Skoog, D. A., West, D. M. and Holler, F. J., *Fundamentals of analytical chemistry.* College Publishing, Philadelphia, **1992.**

[16]APHA, AWWA and WEF., *Standard Method for the Examination of water and waste water, 20th ed. Am. Pub. Health. Ass. Washington D.C.* **1998.**

[17]Alper, B., Abidin, K. and Yuksel, K. B., *Water, Air Soil Pollut.*, **1998**, *149,* 93–111.

[18]Dalmacija, B., *Water Quality Control in Towards of Quality Management, Novi Sad,* **2000.**

[19]Stat Soft, Inc. STATISTICA (data analysis software system), ver. 6. http://www.statsoft.com. **2001.**

[20]Tukey, J. W., *Exploratory data analysis*. Addison-Wesley. Reading, **1977.**

[21]Davis, M. and Masten, S., *Principles of Environmental Engineering and Science*, *The McGraw Hill Company, New York,* **2002.**

[22]Environment Protection Agency (EPA), US Environment Protection Agency: *Safe drinking water act amendment*. **2002**.

[23]Osuinde, M. I. and Eneuzie, R., *Nigerian J. Microbiol*., **1999**, *13,* 47-54.

LIPID PROFILE AND FATTY-ACID COMPOSITION OF HUMAN SERUM IN HYPERTENSION PATIENTS

Mohamed A. H. Jasim[a]

Keywords: Hypertension, fatty acids, cholesterol ester, phospholipids, triglyceride.

The aim of this study was designed to determine the effect of hypertension on the level of lipid fractions and percentage of fatty acids in serum. The study included 50 patients with hypertension, blood was taken after 10-12 h fasting. The age of patients was between 60 and 80 years. Blood samples from (50) normal subject with the same age were collected as control. The patients samples collection were from the medical word. A number of biochemical parameters were measured using enzymatic kits methods also the analysis and the measurement of percentage of fatty acids in fatty component of serum (cholesterol ester (CE), phospholipids (PL) and triglyceride (TG)) separated by thin layer chromatography(TLC) followed by transmethylation of fatty acids and measurement of fatty acids percentage using Capillary Gas Chromatography (CGC). The result of this study showed that there is a significant differences in the level of studied biochemical parameters and fatty acids percentage in hypertension patients compared with the control group. The results of this study also showed that a significant increase in level of (TG) in serum of hypertension patients. The result showed that a significant increase in percentage of (PUFA) in (PL) part.

Corresponding Author
  E-Mail: m.7186@yahoo.co.uk
[a] Chemistry Department, College of Education, Mosul
  University, Mosul, Iraq

Introduction

Dietary fatty acid intake may affect blood pressure. Some studies have found that saturated fats increase blood pressure and that polyunsaturated and monounsaturated fats decrease blood pressure. Many of the studies that have examined the relation between fatty acids and blood pressure have measured or manipulated the dietary intake of fatty acids. Because the methodologies that assess dietary intake are imprecise, alternative methods of estimating fatty acid intake have been proposed. Dietary-derived essential fatty acids that may be associated with blood pressure can be precisely measured in the cholesterol esters and phospholipids of serum lipoproteins.[1] The nonessential fatty acid composition of cholesterol esters and phospholipids reflect dietary consumption as well as fatty acid synthesis and metabolism and therefore are less reliable indicators of dietary intake. Nevertheless, the associations with blood pressure of individual saturated fatty acids, such as myristic acid (14:0), palmitic acid (16:0), and stearic acid (18:0), which are highly correlated in the diet may be examined with the use of serum fatty acid levels.[2]

To examine the association between serum fatty acids and blood pressure, we conducted a cross-sectional study of men enrolled in the Multiple Risk Factor Intervention Trial (MRFIT).[3] Using stored frozen serum samples that were collected at the outset of the study, we measured the serum fatty acid levels in fifty patients and fifty control subjects. We have performed stepwise multivariate analyses to determine whether serum fatty acids were independently associated with blood pressure.

Experimental

Collection and treatment of blood samples

In this study the blood samples were collected from hypertension patients and control subjects over a period between 9/12/2008 and 23/2/2009, after fasting for 10-12 h. Blood (5 mL) was collected from each subject and then the serum was separated. Serum was divided into two parts. From one part, total cholesterol (TC), high density lipoprotein cholesterol (HDL-C), triglyceride (TG), low density lipoprotein cholesterol (LDL-C) were measured by enzymatic methods using kits.[4,5] Very low lipoprotein cholesterol (VLDL-C) was evaluated theoretically.[6] The second part was stored at -18 °C for the measurement of fatty acids.

Serum samples were treated with methanol and chloroform to extract lipids.[7] Lipids extract was separated into three parts cholesterol ester (CE), TG and phospholipids (PL) by TLC.[8] Analysis and re-esterification of fatty acids were achieved using boron trifluoride(BF$_3$)(16 %) in methanol.[9] Determination of fatty acids in the three lipid fractions was performed by Capillary Gas Chromatography (CGC) Shimadzu 2010, column type TR-WAX, and length 30 m.

Statistical analysis of results from biochemical parameters and percentage of fatty acids was performed using T-test, p≤0.05 was considered significant.[10]

Results

Lipid Fraction

The results presented in Table 1 showed significant increase in TC (p<0.05), LDL-C (p<0.001), TG (p<0.001) and VLDL-C (p<0.001) in the patient group in comparison

with those of the control group. On the other hand, the results showed significant decrease in HDL-C.

Percentage of fatty acids

The percentage of fatty acids was measured using CGC through comparison of results with standard sample composed of twelve fatty acids. Retention time (RT) of the standard fatty acids is given Table 2.

Table 1. Serum lipids from patient and control groups.

Lipid fraction mmol L^{-1}	Control $n = 50$	Hypertension patient $n = 50$	P value
TC	4.80±0.31	5.01±0.80	≤0.05
HDL-C	1.48±0.10	0.80±0.10	≤0.05
LDL-C	2.80±0.25	3.21±0.23	≤0.001
TG	1.19±0.10	3.40±0.46	≤0.001
VLDL-C	0.28±0.03	1.20±0.35	≤0.001

Table 2. Retention time of standard fatty acids.

Standard fatty acids	Symbol	Retention time (min)
Capric acid	C10:0	4.900
Lauric acid	C12:0	5.138
Myristic acid	C14:0	8.500
Palmitic acid	C16:0	10.08
Palmitoleic acid	C16:1	16.74
Stearic acid	C18:0	19.09
Oleic acid	C18:1	19.48
Linoleic acid	C18:2	20.12
Linolenic acid	C18:3	22.20
Arachidonic acid	C20:4	23.46
Eicosapentaenoic acid	C20:5	25.12
Docosahexaenoic acid	C22:6	26.68

The results of the determination of fatty acids in the patient and control groups showed that there is no significant increase in percentage of total saturated fatty acids (SFA), whereas significant increase in total percentage of monounsaturated fatty acids (MUFA) and polyunsaturated fatty acids (PUFA) in the patient group in comparison with control group in the CE part. Also the results showed that a significant decrease in total of SFA and MUFA and a significant increase in total of PUFA in the patient group in comparison with control group in the PL part. The result presented in Table 3 showed that a significant increase in total of SFA and MUFA, and significant decrease in total of PUFA in the patient group in comparison with the control group in TG.

Discussion

Lipid Fractions

The results showed that there is a significant increase in TC in the patient group as compared with that of control group (Table 1). This may well be due to an increase in TC

synthesis as a result of insulin resistance in patients.[11] The results also showed that a significant decrease in HDL-C in the patient group in comparison with the control group, which may be due to a close relationship to the elevated activity of plasma cholesterol ester transfer protein which promotes the lipoprotein cholesterol of HDL to be transferred to other lipoprotein in patients.[12] The observed significant increase in LDL-C may be due to a defect in hepatic receptor, Apo B100, which plays an important role in increasing LDL-C through decreasing transport of LDL-C to hepatic tissue.[13]

The result of this study indicate that there is a significantly higher level of TG and very low density lipoprotein cholesterol in the patient group as compared those in the control group. It may be either due to decrease in lipoprotein lipase activity in hypertension patients which leads to decrease in TG clearance from blood[14] or due to insulin resistance in hypertension patients which causes abnormality in metabolism of lipids.[15]

Fatty acids in CE fraction

The results of this study indicate that there was no significant difference in the percentage of saturated fatty acids between that in the patient and control groups. Further, there is a significant increase in the total percentage of monounsaturated and polyunsaturated fatty acids. This may be due to an abnormality in action of lipoprotein lipase which leads to a defect in metabolism of TG and lead to increase percentage of fatty acids.[16]

Fatty acids in PL fraction

The results of this study showed that there is a significantly lower percentage of total SFA in the patient group as compared that in the control group. It may due to an increased ingestion of some type of food which leads to increase the in the risk factor in the patient group in comparison with control group.[17] This study also showed a significantly lower percentage of total MUFA and a significantly higher percentage of total PUFA for the patient group as compared to those of the the control group. It may be due to insulin resistance in hypertension patients and cardiac disease in general which leads to a big defect in enzymes action specially lipoprotein lipase and also defect in action for enzymes of desaturase class and elongation and oxidation process of fatty acids.[1]

Fatty acids in TG fraction

The result of this study indicate that there is a significant increase in the percentage of total SFA in the TG fraction. It may be due to transport of Acetyl-CoA from different metabolism pathways to the pathway causing anabolism of SFA.[18]

The results showed that there was a significant increase in percentage of total MUFA and a significant decrease in percentage of total PUFA. It may be due to a defect in the action of desaturation enzymes (Δ9), (Δ6), (Δ5) and elongation enzymes in stroke patients.[19]

Table 3. Percentage of fatty acids composition of CE, PL and TG in the patient and control groups.

Fatty acid	CE		PL		TG	
	Control	**Patients**	**Control**	**Patients**	**Control**	**Patients**
N	**10**	**10**	**10**	**10**	**10**	**10**
SFA						
10:0	1.2±0.23	0.98±0.05	0.80±0.01	0.10±0.08	0.55±0.01	0.9±0.08
12:0	0.88±0.31	1.22±0.02	1.2±0.02	1.55±0.05	0.78±0.20	1.88±0.5
14:0	0.72±0.20	0.78±0.10	0.25±0.1	0.28±0.10	2.0±0.05	2.0±0.08
16:0	11.45±1.5	11.51±1.0	26.5±1.5	22.5±1.89	25.5±0.60	27.0±1.8
18:0	1.35±0.27	1.56±0.35	15.8±1.2	12.8±1.52	6.80±0.24	8.0±0.63
Total	15.5±2.50	15.82±1.5	44.05±2.8	37.13±3.6*	35.53±1.0	39.3±3.1*
MUFA						
16:1	3.88±2.24	4.21±1.24*	1.20±0.5	0.8±0.45*	2.25±0.15	4.1±1.0*
18:1	19.20±3.0	21.58±2.2*	9.50±1.2	7.21±0.97*	30.26±1.2	33.5±1.5*
Total	23.08±5.2	25.79±3.5*	10.7±1.70	8.01±1.42*	32.5±1.36	37.6±2.5*
PUFA						
18:2 n-6	38.0±1.0	49.23±4.2*	28.0±1.8	32.02±3.2*	18.0±2.0	14.0±.51*
18:3 n-3	0.45±0.12	0.40±0.15	1.8±0.56	1.95±0.23	2.10±0.45	2.89±.90
20:4 n-6	8.5±1.80	10.15±1.7*	10.62±2.1	12.75±2.0*	1.85±0.05	2.06±.30*
20:5 n-3	1.20±0.2	1.58±0.01	1.56±0.62	1.24±0.25	2.00±0.12	1.05±.01*
22:6 n-3	0.50±0.02	0.85±0.12	4.0±1.10	6.2±1.10*	3.25±0.95	1.20±.20*
Total	50.65±3.1	58.21±6.2*	39.98±6.2	48.16±6.7*	27.2±3.57	21.2±1.9*
n-3	2.15±0.34	2.83±0.28	7.36±2.28	9.39±1.58*	7.35±1.52	5.14±1.1*
n-6	48.5±2.80	55.38±5.9*	32.6±3.90	38.77±5.2*	19.85±2.0	16.06±.8*

*P value ≤ 0.05

Conclusions

High level of triglyceride is linked to atherosclerosis. Condition in which cholesterol and other substances from plaque fragment or blood clots that can bloke the flow of blood in an artery supplying either to the heart, which could cause a heart attack, or to brain, which could cause a stroke. The results of this study showed that there is a in decrease proportion of total SFA and MUFA, and an increase in the proportion of total PUFA. This indicates that there may be an increase in the lipids peroxidation in hypertension patients also an increase in the metabolism of MUFA to PUFA, which considered as a risk factor for stroke because it increases the amount of free radicals.

References

[1]Tabara Y., Takahashi Y., Kawaguchi T., Setoh K., Terao C., Yamada R., Kosuqi S., Sekine A., Nakayama T., Matsuda F., *Hypertension*, **2014**, *64*, 1212.

[2]Guo S. X., Yang Z. M., Zhang J. Y., Guo H., Zhang Y. H., Xu, S. Z., *Chin. J. Hypertens.*, **2010**, *18*, 459.

[3]Mcgarry, J. D., *Diabetes*, **2002**, *51*, 7.

[4]Burtis, C., Ashwood, E., *Tietz Text Book of Clinical Chemistry*, 3rd edition, Elsevier, Amsterdam, **1999**, 110.

[5]Kosnor, G. M, *Clin. Chem.*, **1976**, *22*, 665.

[6]Michael, L, Edward P, Larry S., *Clinical Chemistry,* 5th edition, Williams & Wilkins, Philadelphia, **2005**, 288.

[7]Folsom, A., Ma J. E., *J. Metabolism*, **1996**, *45*, 223.

[8]Murray R., Gramner, D., Rodweu, V., *Harpers Biochemistry,* 25th ed., Appleton and Lange, New York, **2000**.

[9]Ma J., Shahar, E., *Am. J. Clin. Nutr.*, **2005**, *62*, 564.

[10]Leonard T., Kathleen R., *The ways and means of statistics*, Harcourt Brac Jovanovich, San Diego, **1990,** 490.

[11]Faraj M., Ling H., Katherine C., *Biochem. Cell Biol.*, **2014**, *82*, 175.

[12]Freire R., Cardose A., Ferreria S., *Diabetes Care*, **2010**, *28*, 1770.

[13]Vessby B., Boberg M., Andersson A., *Ann. Acad. Sci.*, **2002**, *967*, 180.

[14]Guo, H., Guo S. X., Zhang J. Y., Ma R. L., Rui D. S., Xu S. Z., Sun F., Hu A. R., Yang Z. M., *Chin. J. Epidemiol.*, **2010**, *31*, 747.

[15]Tanne S., David A., *Circulation*, **2011**, *104*, 24.

[16]Guo, S. X., Yang, Z. M., Zhang J. Y., Guo, H., Zhang, Y. H., Xu, S. Z., Niu, J.-Y., *Chin. J. Hypertens.,* **2010**, *18*, 459–464.

[17]Boden G. O., *Curr. Opin. Endocrinol. Diabetes Obes.*, **2011**, *18*, 139.

[18]Fukuchi S., Hamaguchi K., Seike M., *Exp. Biol. Med.,* **2011**, *229*, 480.

[19]Iso H., Sato S., *Stroke,* **2008**, *33*, 2086.

PHASE POLYMORPHISM OF [M(OS(CH₃)₂)₆](ClO₄)₂ (M=Mn(II) AND Zn(II) STUDIED BY TRANSMITTED LIGHT INTENSITY AND POLARIZED OPTICAL MICROSCOPY MEASUREMENTS

E. Szostak[a]*, A. Migdał-Mikuli[a], J. Chruściel[b] and A. Rudzki[b]

The transmitted light intensity (TLI) and polarized optical microscopy (POM) measurements of [Mn(OS(CH₃)₂)₆](ClO₄)₂ and [Zn(OS(CH₃)₂)₆](ClO₄)₂, as a function of temperature, showed that only some of the phase transitions discovered earlier for these compounds by the differential scanning calorimetry were now observed as anomalies on the TLI curves and as different textures in POM pictures. Above-mentioned methods indicated that discovered phases of both compounds were the crystalline phases with different orientational dynamical disorder. Additionally, it was confirmed that these both compounds melt at 488 and 465 K, respectively.

Corresponding Authors
ax: +48 12 664 0515
E-Mail: szostak@chemia.uj.edu.pl
[a] Faculty of Chemistry, Jagiellonian University, ul. Ingardena 3, 30–060 Kraków, Poland,
[b] Faculty of Sciences, Siedlce University of Natural Sciences and Humanities, ul. 3 Maja 54, 08-110 Siedlce, Poland,

Introduction

Physicochemical properties of coordination compounds of [M(OS(CH₃)₂)₆]X₂, type containing DMSO ligands have been the subject of research studies for a long time.[1-10] These studies have revealed very rich and interesting phase polymorphism of these substances. The number and type of the phase transitions depends on the chemical nature of the cation and anion, as well as on so-called "thermal history" of the sample. In this article, we will present some new results obtained for [Mn(OS(CH₃)₂)₆](ClO₄)₂ and [Zn(OS(CH₃)₂)₆](ClO₄)₂.

At room temperature [Mn(OS(CH₃)₂)₆](ClO₄)₂ crystallizes in the orthorhombic system (Fdd2 space group, No. = 43) and [Zn(OS(CH₃)₂)₆](ClO₄)₂ in the trigonal system (P3₁c space group, No. = 159), with eight and two molecules in an elementary unit cell, respectively.[11,12] They are isostructural with [Cd(OS(CH₃)₂)₆](ClO₄)₂ and [Ni(OS(CH₃)₂)₆](ClO₄)₂ compounds, respectively.[1,6] We have recently investigated the polymorphism of the above mentioned compounds ([M(DMSO)₆](ClO₄)₂, where M = Cd, Ni Mn, Zn) using differential scanning calorimetry (DSC) and have found that they have at least four higher temperature polymorph phases.[1,3,4,6] Some of these phases can be very easily overcooled to form metastable states. The orthorhombic compounds show an additional phase transition below room temperature. At this phase transition the crystal structure of these compounds changes from orthorhombic to monoclinic. Compounds which crystallize in the trigonal system do not show any low temperature phase transitions.

In this work transmitted light intensity (TLI) and polarized optical microscopy (POM) measurements were performed to follow the nature (phase transition or changes in molecular dynamics) of transitions detected in our earlier DSC experiments in the temperature range of 273–473 K.

EXPERIMENTAL

Sample Preparation

All measured samples were prepared and their chemical composition were determined by the methods described previously.[3,4,13] The chemical identity and purity of the examined compounds have been also confirmed by Fourier transform Raman scattering (FT-RS) and infrared absorption (FT-IR) spectra and additionally by thermal analysis methods (TG + QMS and SDTA).[3,4]

Transmitted Light Intensity and Polarized Optical Microscopy measurements

The TLI measurements were made using Dresden Analitik polarizing microscope with a home-made set-up, equipped with Burr-Brown photodiode OPT101 (source of light, polarizing microscope, detector - photodiode and recorder), the heating stage and the temperature controller were the same as in POM measurements.

The POM measurements were carried out using Nicon polarizing microscope Eclipse E200 equipped with Linkam heating stage THMSE 600 and temperature controller TMS 93 and digital camera DG-01 (CHUGAI BOYEKI).
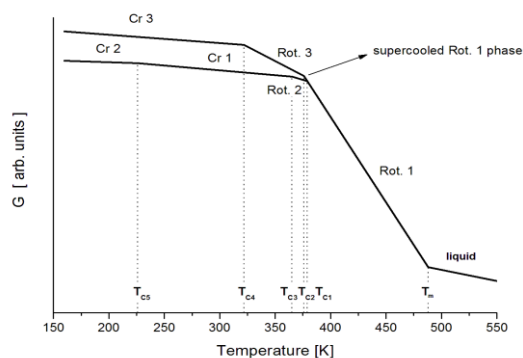
RESULTS AND DISCUSSION

[Mn(OS(CH₃)₂)₆](ClO₄)₂

The thermodynamic parameters obtained for phase transitions of [Mn(DMSO)₆](ClO₄)₂ by our earlier DSC measurements and the schematic representation of the Gibbs free energy (G)-temperature relationship are given in Table and Figure 1, respectively.

Table 1. Thermodynamics parameters of the phase transitions detected in [Mn(OS(CH₃)₂)₆](ClO₄)₂.[3]

	Heating			Cooling		
	$\Delta T \pm S_{\Delta T}$, K	$\Delta H \pm S_{\Delta H}$, kJ·mol⁻¹	$\Delta S \pm S_{\Delta S}$, J·mol⁻¹·K⁻¹	$\Delta T \pm S_{\Delta T}$, K	$\Delta H \pm S_{\Delta H}$, kJ·mol⁻¹	$\Delta S \pm S_{\Delta S}$, J·mol⁻¹·K⁻¹
T_m	488 ± 3	37.83 ± 1.30	184.5 ± 1.7	–	–	–
T_{c1}	379 ± 1	3.43 ± 0.40	9.1 ± 1.1	–	–	–
T_{c2}	376 ± 2	4.44 ± 0.45	11.8 ± 1.2	370 ± 2	5.27 ± 0.4	14.2 ± 1.2
T_{c3}	365 ± 3	27.11 ± 1.24	74.3 ± 2.9	–	–	–
T_{c4}	322 ± 3	16.60 ± 0.62	51.6 ± 1.8	315 ± 4	16.4 ± 0.8	52.0 ± 2.3
T_{c5}	225 ± 1	0.88 ± 0.11	2.0 ± 0.3	223 ± 1	0.8 ± 0.2	1.9 ± 0.5

The sample without "thermal history" contains the crystalline phase called Cr 1. The TLI measurements were started by heating of this sample from room temperature (RT) up to 393 K. Upon heating the sample a phase transition was occurred when the Cr1 phase was transformed into the intermediate Rot. 2 phase at T_{C3} = 365 K (see Figure 2 and compare it with Figure 1). Due to this transition, a distinct anomaly on TLI curve was recorded, which could be related to significant decreasing of the transmitted light intensity.

During further heating of the sample, the phase Rot. 2 was transformed into the high temperature Rot. 1 phase at T_{C1} = 379 K, which was manifested in a very small anomaly on TLI curve.

Figure 1. Scheme of the temperature dependence of free enthalpy *G* for [Mn(OS(CH₃)₂)₆](ClO₄)₂.
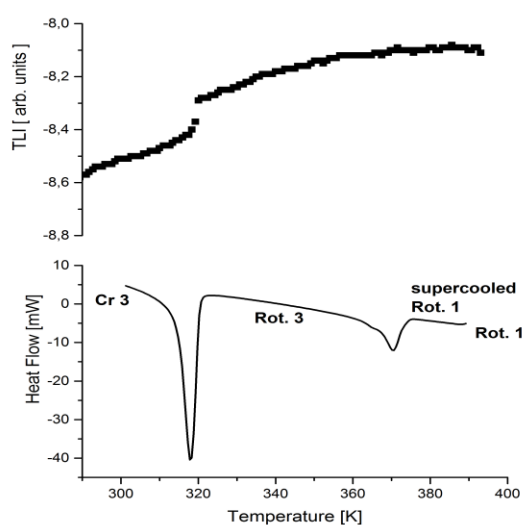
Figure 3. Differential scanning calorimetry and transmitted light intensity curves obtained during cooling [Mn(OS(CH₃)₂)₆](ClO₄)₂ from 393 to 298 K.
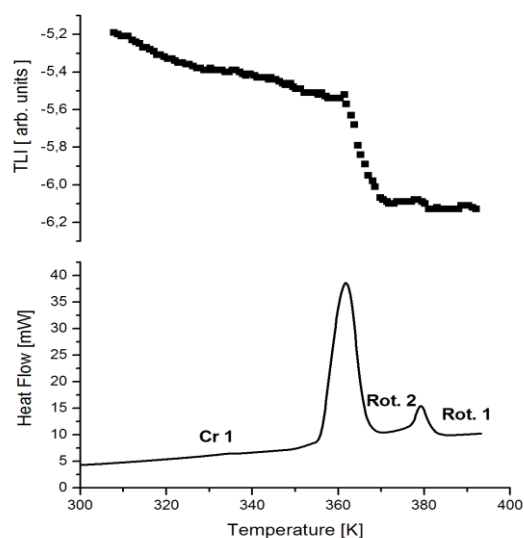
Figure 2. Differential scanning calorimetry and transmitted light intensity curves obtained during heating [Mn(OS(CH₃)₂)₆](ClO₄)₂ from 300 to 393 K.
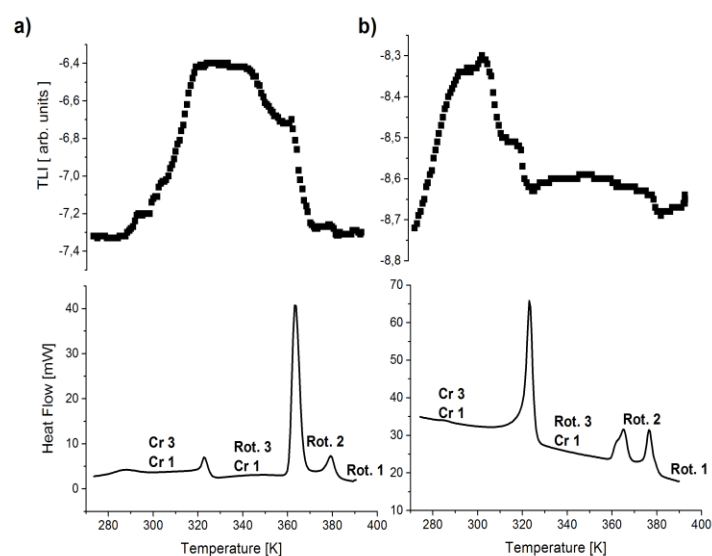
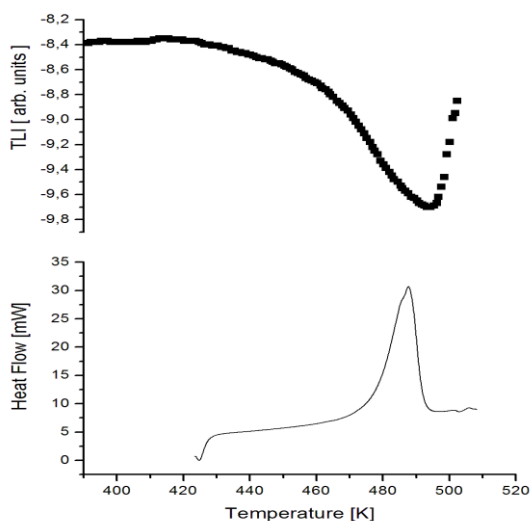**Figure 4.** Differential scanning calorimetry and transmitted light intensity curves obtained during heating [Mn(OS(CH₃)₂)₆](ClO₄)₂ from 270 to 393 K.

Figure 5. Differential scanning calorimetry (DSC) and transmitted light intensity curves obtained during heating [Mn(OS(CH₃)₂)₆](ClO₄)₂ from 393 to 510 K.

Cooling the sample Rot. 1 phase from 393 K to 298 K, results in a phase that is slightly supercooled. The supercooled Rot. 1 phase undergoes a phase transition at T_{C2} = 370 K into the metastable phase Rot. 3. However, this transition does not change the transmitted light intensity. Being further cooled down, the Rot. 3 phase goes into the Cr 3 phase at T_{C4} = 315 K (see Figure 3 and compare it with Figure 1).

The phase transition at T_{C4} was observed on the TLI curve as an anomaly connected to an insignificant decrease of the transmitted light intensity. It is known from our previous DSC measurements that when the heating speed is high the phase transition from the supercooled Rot. 1 phase to the Rot. 3 phase (at T_{C2}) and the transition from the Rot. 3 phase into the Cr 3 phase (at T_{C4}) are reversible transitions,[3] however, when the heating is slow, the phases Rot. 3 and Cr 3 convert into stable phase Cr 1. It is clearly visible in Figure 4 a and b, which show the TLI curves, recorded during heating the sample in a temperature range 273-393 K with a rate of 2 K min⁻¹. The observed initially increase of the transmitted light intensity on TLI curve is probably attributed to a relatively slow spontaneous conversion of the metastable Cr 3 phase into the stable Cr 1 phase. This process might be taken as an analogue of a new phase crystallisation.[14] On further heating, the rest of the Cr 3 phase undergoes a phase transitions into the phase Rot. 3 and supercooled Rot 1. At the end, stable phase Cr 1 undergoes a phase transition into the stable Rot. 1 phase at the temperature T_{C1} = 379 K. The DSC curves presented in Figure 4, below the TLI curves, show the possible ways of spontaneous conversion of these polymorphs into the stable phase Cr 1.

Heating up the hermetically closed sample above the T_{C1} temperature, the sample melts at T_m = 488 K. As it can be seen in Figure 5, the TLI curve unambiguously shows the anomaly resulting from the melting process. Table 2 indicates the phase transitions registered as anomalies on TLI curves associated with a change of the sample texture.

The textures of [Mn(OS(CH₃)₂)₆](ClO₄)₂ at different phases were recorded using POM in a function of temperature and presented in Figure 6. Measurements were

conducted with the scanning rate of 10 K min⁻¹ in four steps. At first, the sample was cooled down from 293 to 203 K. In two next steps, the sample was heated up to 393 K and then cooled down to 273 K. In the last step the sample was heated up to 486 K. As can be seen in Figure 6, the greatest differences between POM textures were registered for solid Cr 1, Rot. 2 and Rot. 1 phases (Figures 6b-6d)). Moreover some small changes in the brightness and sharpness of POM textures of Rot 3 and Cr 3, and Cr 2 and Cr 1 phases were also observed (Figures 6e, 6f and 6a, 6b).
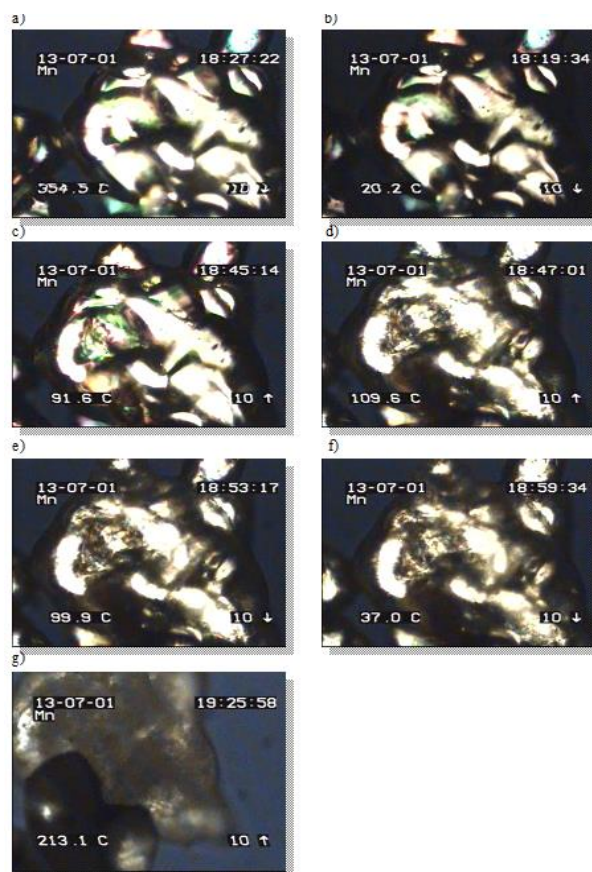
Figure 6. [Mn(OS(CH₃)₂)₆](ClO₄)₂ crystal images obtained using POM at the temperature: a) 218 K – phase Cr 2, b) 293 K – phase Cr 1, c) 365 K – phase Rot. 2, d) 383 K – phase Rot. 1, e) 373 K – phase Rot. 3, f) 310 K – phase Cr 3 and g) 486 K – liquid.

Heating of the sample above 393 K causes melting of Rot. 1 phase at ca. 486 K. This transition was registered in the last step of POM measurement. The view of liquid form of [Mn(OS(CH₃)₂)₆](ClO₄)₂ compound was presented in Figure 6g.

Table 2. Phase transitions of [Mn(DMSO)₆](ClO₄)₂ detected by TLI method

	Heating	Cooling
T_C		
T_m	+	−
T_{C1}	+	−
T_{C2}	−	−
T_{C3}	+	−
T_{C4}	+	+
T_{C5}	−	−

The phase transitions observed by both DSC and TLI methods are denoted as "+". The phase transitions which were observed by DSC but could not be observed by TLI method are denoted as " − ".

Table 3. Thermodynamics parameters of the phase transitions detected in [Mn(OS(CH₃)₂)₆](ClO₄)₂.[3]

	Heating			Cooling		
	$\Delta T \pm S_{\Delta T}$, K	$\Delta H \pm S_{\Delta H}$, kJ·mol⁻¹	$\Delta S \pm S_{\Delta S}$, J·mol⁻¹·K⁻¹	$\Delta T \pm S_{\Delta T}$, K	$\Delta H \pm S_{\Delta H}$, kJ·mol⁻¹	$\Delta S \pm S_{\Delta S}$, J·mol⁻¹·K⁻¹
T_{m2}	456 ± 3	21.42 ± 0.82	47.0 ± 2.1	–	–	–
T_{m1}	389 ± 2	7.63 ± 0.23	19.6 ± 0.6	386 ± 1	7.48 ± 0.14	19.4 ± 0.4
T_{c1}	355 ± 1	25.33 ± 0.69	71.4 ± 1.9	–	–	–
T_{c2}	341 ± 1	2.37 ± 0.30	7.0 ± 0.9	–	–	–
T_{c3}	315 ± 1	21.31 ± 3.15	67.7 ± 10.3	309 ± 1	18.80 ± 5.62	60.8 ± 18.2

[Zn(OS(CH₃)₂)₆](ClO₄)₂

The thermodynamic parameters obtained for phase transitions of [Zn(DMSO)₆](ClO₄)₂ based on our earlier DSC measurements and the schematic representation of the Gibbs free energy (*G*)-temperature relationship are given in Table and Fig. 1, respectively.[4]
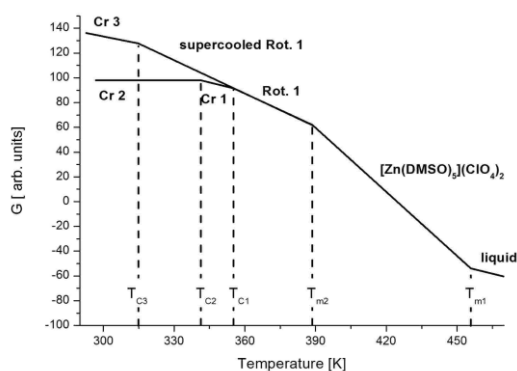
Figure 7. Scheme of the temperature dependence of free enthalpy *G* for [Zn(OS(CH₃)₂)₆](ClO₄)₂.

The measurements were started by heating the sample from room temperature (RT) to 373 K. While heating the sample, being initially in the Cr 2 phase, the phase transition into intermediate phase which was named Cr 1 can be observed on DSC curve at T_{C2} = 341 K (see Fig. 8). This transition was not registered on the TLI curve what suggests that it is no connected with changing of the sample texture. Phase Cr 1 next transforms at T_{C1} = 355 K into the high temperature phase, named Rot. 1, that is manifested as a big anomaly on the DSC curve and small anomaly on the TLI curve.

Cooling of the sample being in Rot. 1 phase may happen in two different ways. In the first case the Rot. 1 phase transforms into the Cr 2 phase which next transforms into the Cr 1 phase. In the second case phase transition occurs between the supercooled Rot. 1 and metastable Cr 3 phase. As seen by the DSC measurements usually during this process metastable Cr 3 phase transforms exothermically into the stable Cr 1 phase (see the DSC curve in Figure 9).
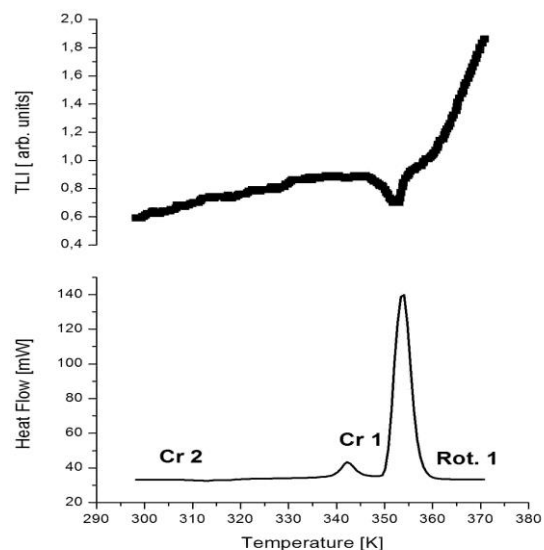
Figure 8. DSC and TLI curves obtained during heating [Zn(OS(CH₃)₂)₆](ClO₄)₂ from 298 to 373 K.
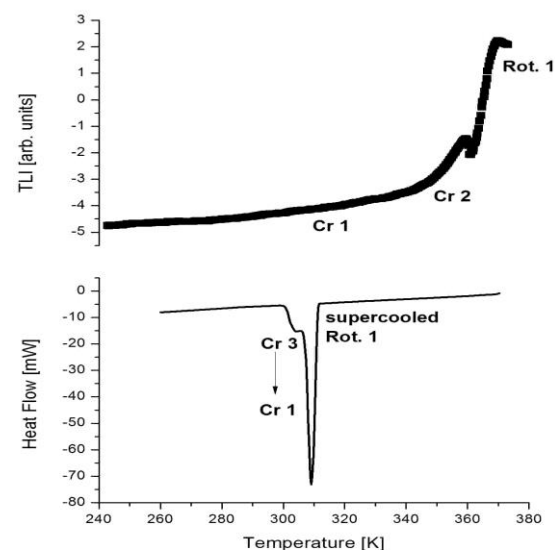
Figure 9. DSC and TLI curves obtained during cooling [Zn(OS(CH₃)₂)₆](ClO₄)₂ from 373 to 240 K.

Phase transitions between phases: Rot. 1 ↔ Cr 2 ↔ Cr 1 were not recorded on the DSC curve but are clearly visible on the TLI curve (see the TLI curve in Fig. 9).

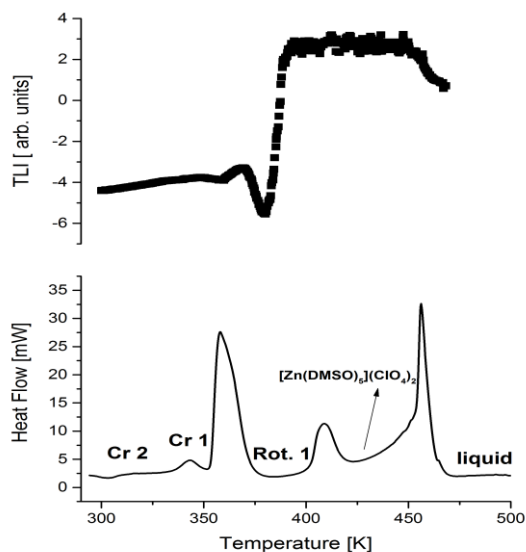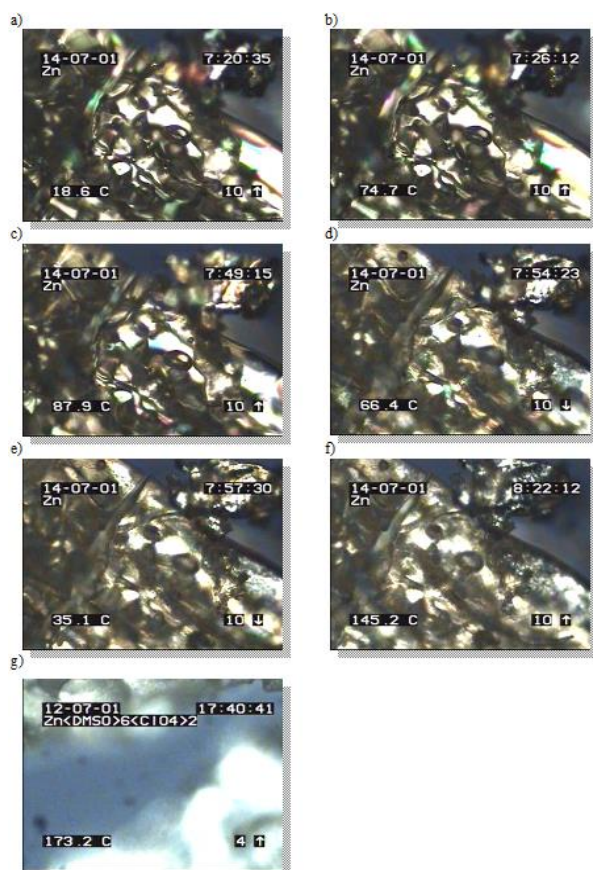**Figure 10.** DSC and TLI curves obtained during heating $[Zn(OS(CH_3)_2)_6](ClO_4)_2$ from 298 to 500 K.

Figure 11. $[Zn(OS(CH_3)_2)_6](ClO_4)_2$ crystal images obtained using thermal microscope at the temperature: a) 292 K – phase Cr 2, b) 348 K – phase Cr 1, c) 361 K – phase Rot. 1, d) 339 K – supercooled phase Rot. 1, e) 308 K – phase Cr 3, f) 418 K – $[Zn(OS(CH_3)_2)_5](ClO_4)_2$ crystal and g) 446 K – liquid.

Second heating of the sample from 300 K to 373 K gives similar results as registered before both on DSC and TLI curves. During further heating above the T_{C1} temperature, hermetically closed sample partially melts at $T_{m2} = 389$ K, and then it completely melts at $T_{m1} = 465$ K. All mentioned above phase transitions are connected with the change of the intensity of the transmitted light (see Figure 10).

To observe of all the phases occurring in $[Zn(OS(CH_3)_2)_6](ClO_4)_2$, the POM measurements at different temperature were conducted in five steps. In the first step, the sample was heated from 273 to 348 K and then cooled down from 348 to 243 K. In two next steps, the sample was heated in the temperature range of 243-375 K and cooled in the range of 375-243 K. In the last step the sample was heated from 243 up to 453 K.

Table 4. Phase transitions of $[Zn(DMSO)_6](ClO_4)_2$ detected by TLI method

	Heating	**Cooling**
T_C		
T_{m1}	+	−
T_{m2}	+	−
T_{C1}	+	+/−
T_{C2}	−	−
T_{C3}	−	−

The phase transitions observed by both DSC and TLI methods are denoted as "+". The phase transitions which were observed by DSC but could not be observed by TLI method are denoted as "–". The "+/-" this transition was only observed by TLI method.

Figure 11 presents the POM textures of all phases which were detected earlier by DSC method[4]. As can be seen in this figure the most significant differences between POM textures were obtained for the phases: Cr 1 and Rot 1 (Figures 6(b, c), Rot 1 and $[Zn(OS(CH_3)_2)_5](ClO_4)_2$ crystal (Figures 6(c, f), $[Zn(OS(CH_3)_2)_5](ClO_4)_2$ crystal and liquid (Figures 6(f, g). Table 4 indicate which of the phase transitions registered as anomalies on TLI curves are associated with a change of the sample texture.

CONCLUSIONS

1. The TLI measurements performed in a function of temperature showed that not all of the phase transitions observed earlier by the DSC method for $[Mn(OS(CH_3)_2)_6](ClO_4)_2$ and $[Zn(OS(CH_3)_2)_6](ClO_4)_2$ were observed as anomalies on the TLI curves. These anomalies can be associated with a change of the sample texture.

2. The POM observations performed in a function of temperature indicated only small differences between some pictures confirmed that all phases of $[Mn(OS(CH_3)_2)_6](ClO_4)_2$ and $[Zn(OS(CH_3)_2)_6](ClO_4)_2$, investigated earlier by the DSC method, are the crystalline phases, and that these crystals melt at ca. 488 and 465 K, respectively.

3. DSC, TLI and POM measurements indicated that discovered phases of both compounds were the crystalline phases with different orientational dynamical disorder.

References

[1]Migdał-Mikuli, A., Mikuli, E., Szostak, E., Serwońska J., *Z. Naturforsch.* **2003,** *58a*, 341-345.

[2]Migdał-Mikuli, A., Szostak, E., *Thermochim. Acta.* **2005,** *426*, 191-198.

[3]Migdał-Mikuli, A., Szostak, E., *Z. Naturforsch.* **2005,** 60a, 289-295.

[4]Migdał-Mikuli, A., Szostak, E., *Thermochim. Acta.* **2006***, 444,* 195-200.

[5]Migdał-Mikuli, A., Skoczylas, Ł., Szostak, E.., *Z. Naturforsch.* **2006**, 61a, 180-188.

[6]Migdał-Mikuli, A., Szostak, E., *Z. Naturforsch.* **2007***, 62a,* 67-74.

[7]Migdał-Mikuli, A., Szostak, E., Drużbicki, K., Dołęga, D., *J. Therm. Anal. Calor.* **2008,** 93, 853-856.

[8]Migdał-Mikuli, A., Skoczylas, Ł., Szostak, E., *J. Coord. Chem.* **2008**, *61,* 2197-2206.

[9]Szostak, E., Migdał-Mikuli, A., *J. Therm. Anal. Calor.* **2010** 101, 601-606.

[10]Migdał-Mikuli, A., Szostak, E., Bernard, P., *J. Therm. Anal. Calor.* **2014,** *115*, 443-449.

[11]Migdał-Mikuli, A., Szostak, E., Nitek, W., *Acta Cryst. E.* **2006,** *62,* m2581-m2582.

[12]Persson, I., *Acta Chem. Scand.* **1982,** *36a,* 7-13.

[13]Cotton, F. A., Francis, R., *J. Am. Chem. Soc.* **1960,** *82(12)*, 2986-2991.

[14]Mnyukh, Y., *Fundamentals of Solid-State Phase Transitions, Ferromagnetism and Ferroelectricity.* Bloomington: 1ˢᵗ Books Library; **2001**.

COMPARATIVE STUDY OF CHEMICAL COMPOSITION OF *CALOTROPIS GIGANTEA* FLOWER, LEAF AND FRUIT ESSENTIAL OIL

Minakshi Singh[a]* and Kalim Javed[a,b]

Essential oil from flowers, leaves and fruits of *Calotropis gigantea* (L), was extracted by hydrodistillation method. Total 21 components in leaves, 43 components in flowers and 21 components in fruits were identified. The extracted oil was characterized by GC and GC-MS techniques. Constituents common to flower, leaves and fruit were 3-hexen-1-ol, benzaldehyde, benzyl alcohol, ± linalool, oct-3-en-2-ol, phenethyl alcohol, α- terpineol, 2,4-dimethylacetophenone, 4-vinylguaiacol and n-tetradecane.

* Corresponding Authors
    E-Mail:- *minakshigaur80@gmail.com*,
    Cell: +91 9891474586
[a]   Department of Chemistry, Mewar University, Chhittorgarh, Rajasthan (India), PIN-312901
[b]   Department of Chemistry, Jamia Hamdard, New Delhi (India), PIN-110062

INTRODUCTION

Calotropis a genus belongs to family of Asclepiadaceae in plant kingdom, consist of six species of perennial shrubs distributed in tropical and subtropical Asia, and Africa.[1] *Calotropis gigantea* is found in Indian subcontinent and have great economic importance.[2] It has great medicinal importance, various parts of this plant is reported to have multiple therapeutic activity. The root bark is used to treat dysentery and elephantiasis, the flowers in small doses gives relief in colds, coughs, asthma, and indigestion[1]. Reported as a indigenous medicine the latex and roots are used in birth control[3] In agriculture leaf extracts are used to protect *Oryza sativa* from pathogenic fungus,[4,5] and in material science to synthesize nanomaterials.[6] Interestingly, as traditional biopesticides the plant is used in controlling mollusks and mosquitoes.[7,8] *Calotropis gigantea* invites attention of the researchers worldwide for its pharmacological activities. Latex contains the cardiac glycosides, calotopin, uscharin, calotoxin, calactin and uscharidin; gigantin and aqueous extract has reported activities such as anti diabetic, antitoxin, antihepatotoxin, antioxidant and wound healing activity. Moreover, variety of chemical groups including cardenolides, steroids, flavonoids, terpenoids, cardiac glycosides, resins, fatty acids and non-protein amino acids etc. have also been identified and reported in *C. gigantea,*[9] which leads to various applications in food, flavour and pharma industries as well as chemical industries to transformed into promising biologically active molecules for chemicals and drugs synthesis. For example, eugenol and guaiacol one of the major constituents of *Calotropis* essential oil, which is recently being explored as a substitute of fossil based chemicals for making biobased materials and green chemicals.[10,11]

Essential oils (EO) are proficient "green" alternative in the pharmaceutical, food and agriculture industries due to the presence of promising chemicals[10,11,15] and effective biological activity.[16]

In the present study, we investigate the essential oil extract of C. gigantea flower, leaf and fruit chemical profiling and comparative evaluation of the chemicals identified by gas chromatography with flame ionisation detection (GC-FID) and gas chromatography with mass spectrometry (GC-MS). This study includes identification of about 21 compounds from the hydrodistilled extract of flower, 43 compounds from leaf and 21 compound from fruit of *C. gigantea*.

MATERIALS AND METHOD

Source of the plant

Fresh flower, leaves and fruit of *Calotropis gigantea* were collected during flowering season from the roadsides (April 2014), dry wasteland area adjacent to Muzaffarnagar (29.4723° N, 77.7089° E) having weather (29 °C, wind at 6 km h^{-1}, 80 % humidity), Uttar Pradesh state, India. Collected plant materials were submitted for identification at National Institute of Science Communication and Information Resources (NISCAIR), New Delhi. A voucher specimen is available in the herbarium division of the NISCAIR.[20]

Isolation of essential oil

Flower, leaves and fruit were washed properly three times with fresh water and dried in shade in properly ventilated room under fan in ambient conditions (27 °C) to prevent loss of essential oil. Dried flower, leaf and fruit were

crushed, weighed and subjected to hydro-distillation using distilled water in Clevenger type apparatus for 4-5 h. The distillated product was further solvent extracted with n-hexane and passed through   anhydrous sodium sulphate to remove residual water. The yield of essential oil obtained was found to be 0.13 % w/w from flower, 0.11 % w/w from leaf and 0.23 % w/w from fruit.

Essential oil composition analysis by Gas Chromatography (GC)/ Mass Spectrometry (MS)

Essential oil composition of *Calotropis gigantea* was analyzed using Shimadzu GC -2010 equipped with flame ionization detector using Rtx-5MS (30 m x 0.25 mm ID x 0.25 μm) column.

Table 1. Comparative evaluation of components of *Calotropis gigantea* flower, leaves and fruit.

RT	Component	Flower (Area %)	Leaf (Area %)	Fruit (Area %)
6.02	Furfural	2.39	-	-
6.07	2-Furancarboxaldehyde	-	2.50	-
6.80	3-Hexen-1-ol	0.53	-	0.30
6.92	4-Methyl-3-penten-1-ol	-	3.83	-
8.45	2-Hexyn-1-ol	-	2.86	-
9.68	Gentanol	-	2.90	-
10.80	Benzaldehyde	0.85	1.88	-
12.22	2-Methyl-6-hepten-1-ol	0.57	-	-
12.27	6-Methyl-5-hepten-2-ol,	-	-	2.89
13.43	(+)-β-citronellene	-	1.39	-
13.67	4-Methyl-1-heptanol	-	4.98	-
14.21	cis- Linalool oxide	-	-	3.29
14.30	Benzyl alcohol	42.89	4.10	-
14.72	Phenylacetaldehyde	-	9.16	-
15.53	trans-Linalool oxide	-	-	0.37
16.86	Guaiacol	-	0.86	-
17.29	3,7-Dimethyl-1,6-octadien-3-ol,	2.53	-	-
17.30	± Linalool	-	0.49	0.34
17.50	Oct-3-en-2-ol	-	1.24	0.50
17.51	3-Thiophenemethanol	0.68	-	-
17.90	Phenethyl alcohol	3.56	2.52	3.41
17.93	2,2,6-Trimethyl-1,4-cyclohexanedione,	-	-	1.95
19.03	Gardenol	-	0.64	-
19.82	(-)-Cis-Myrtanol	-	0.72	-
20.21	α-Terpinene	-	0.84	-
20.78	DL-Menthol	-	0.28	-
21.30	Nerol	-	-	0.83
21.60	α- Terpineol	0.80	0.63	0.14
23.08	2,3-Dihydro-benzofuran	1.94	-	-
23.15	n-Undecane	-	1.65	-
23.35	2,3-epoxygeranyl acetate,	-	-	0.38
23.60	β-Cyclocitral	-	0.55	-
23.91	p-Cymen-7-ol	-	-	0.95
24.00	Isocyclogeraniol	-	0.25	-
24.40	2,4-dimethyl-Acetophenone	1.84	-	3.72
24.41	Ethanone, 1-(2,4,6-trimethylphenyl)-	-	-	2.74
24.57	n-Tridecane	-	-	0.75
24.60	(E)- 3,7-dimethyl-2,6-octadien-1-ol	0.80	-	-
25.70	Dill ether	-	0.46	-
26.97	(E)-Cinnamyl alcohol	0.35	-	-
27.28	2,4-Di-tert-butylphenol	-	-	2.43
27.30	4-vinylguaiacol	15.56	-	3.86
27.82	α-Citral	-	0.06	-
27.95	Heptylidene acetone	-	0.48	-
28.54	Pinocampheol	0.95	-	-
28.60	Artemisia alcohol	-	1.16	-
29.03	Eugenol	-	0.30	-
29.24	2-Methoxy-4-(2-propenyl)phenol,	0.96	-	-
29.46	(Z)-Amylcinnamaldehyde	-	0.96	-
30.22	Spathulenol	-	0.39	-
30.33	3-Phenyl-2-propenoic acid, methyl ester	0.80	-	-

30.50	n-Tetradecane	0.76	0.30	-
31.04	Nerylacetone	-	0.53	-
34.60	Phthalic acid, bis(7-methyloctyl) ester	-	-	0.71
34.68	(E)-β-Ionone	-	1.84	-
34.86	5-Methyl-2-phenylhex-2-enal	-	2.47	-
35.68	Dodecanoic acid, trimethylsilyl ester	-	-	1.07
36.02	Cyclohexyl ketone	-	0.97	-
38.13	Methyl jasmonate	-	0.38	-
38.92	Ribitol, TMS	-	-	1.25
38.98	Trimethylsilyl laurate	-	1.05	-
42.17	5-Methyl-2,4-diisopropylphenol	1.64	-	-
43.45	Phytone	-	0.30	-
45.00	n-Eicosane	0.65	-	-
45.04	Tetradecanoic acid, trimethylsilyl ester	-	-	1.24
46.19	Diisobutyl phthalate	-	-	0.58
48.52	Stearic acid	-	0.67	-
48.74	n-Tetracosane	-	0.71	-
52.29	Phytol	-	17.94	-
52.86	n-Docosane	0.18	-	-

Nitrogen was used as carrier gas at 234.6 kPa inlet pressure. Oven temperature was programmed from 50 ºC for 3.0 minutes, 3.0 ºC min^{-1} to 200 ºC for 2.0 min, 10 ºC min^{-1} to 280 ºC for 7 min. The injector and detector temperature were 250 ºC and 260 ºC respectively. The oil was injected neat with split ratio of 10. Relative amount of individual components are based on GC peak area percentage obtained without FID response factor correction. The retention Indices were obtained from GC by logarithmic interpolation between bracketing n-alkanes. The homogenous series of n-alkanes (C8-C22, Poly Science, Niles, USA) were used as standard.

GC-MS data were obtained on Shimadzu GCMS-QP2010 plus using same chromatographic conditions and column used for GC-FID i.e. Rtx-5MS (30 m x 0.25 mm ID x 0.2 μm column and helium as carrier gas. Temperature programming was 50 ºC for 3.0 mins, 3.0 °C min^{-1} to 200ºC for 2.0 minutes, 10ºC/minutes to 280ºC for 7 minutes.

Identification of constituents

The individual peaks in GC of *Calotropis gigantea* flower, leaf and fruit oil were identified by comparison of their retention indices on the SP Rtx-5MS (30 m x 0.25 mm ID x 0.25 μm) column with literature values[5] and were reported based on its area % response by GC-FID. The essential oil constituents were confirmed by matching of mass spectra of peaks with FFNSC2, NIST08 and Wiley8 library. Identification was done by GC-MS while RI and quantification done by GC-FID.

RESULTS AND DISCUSSION

Chemical investigation of essential oil of traditionally useful *Calotropis gigantea* which is reported for the first time in the literature and identified based on total ion chromatogram (TIC) of oil identified 21 compounds from flower, 43 compounds from leaf and 21 compounds from fruit corresponding to 81.28 %, 81.9 % and 29.9 % total area percentage for flower, leaf and fruit respectively. The yield of essential oil obtained by hydro distillation from *C. gigantea* was 0.13 % (w/w) for flower, 0.11% (w/w) for leaf and 0.23% for fruit oil with respect to their total dry mass. The identified peak comparison is reported in Table 1.

The chemical profiles of the EO reveals the dominance of oxygenated diterpenes (phytol), aromatic alcohol (benzyl alcohol) and linear chain alcohol (4-methyl-1-heptanol) as shown in the Table 1. Among major constituents of essential oil, the major peaks was dominated with benzyl alcohol (42.89 %) and 4-vinylguaiacol (15.56 %) in flower, phytol (17.94 %) in leaf and 4-vinylguaiacol (3.86 %) in fruit. In present study we have identified phenylethyl alcohol (3.56 %, 2.52 %, 3.41 %) and α-terpineol (0.80 %, 0.63 %, 0.14 %) as major constituents in flower, leaf and fruit oil. Benzaldehyde (0.85 %, 1.88 %), benzyl alcohol (42.89 %, 4.10 %) and n-tetradecane (0.76 %, 0.30 %) were identified in flower and leaf oil. ± linalool (0.49 %, 0.34 %) and oct-3-en-2-ol (1.24 %, 0.50 %) were identified in leaf and fruit oil. 4-vinylguaiacol (15.56 %, 3.86 %), 3-hexen-1-ol (0.53 %, 0.30 %) and 2,4-dimethylacetophenone (1.84 %, 3.72 %) were identified in flower and fruit oil.

Phytol and 4-vinylguaiacol are important fragrant ingredient used in many house-hold products including cosmetics, fine fragrances, shampoos, toilet soaps and detergents.[23,24,25] In addition to that, the derivatives of phytol shows crucial pharmacological effects in humans and other animals,[23] while 4-vinylguaiacol can acts as a green source to produce acetovanillone and ethyl guaiacol (used in perfumery) as well as biodegradable polystyrine.[25]

Moreover, a number of other odor-active compounds such as ± linalool (0.49 %), hexanol (0.48 %), α-citral (0.06 %), eugenol (0.30 %) etc. are identified in this study. These minor products are used extensively in chemical industries as perfumery or precursors for making value added products along with some pharmaceutical purposes.[11,26-28] In addition, compounds with strong antimicrobial activity like Benzyl alcohol, p-cresol, and guaiacol have also been identified.

These products can also shows repellent properties against some insects, and thereby being used extensively as important ingredient in insecticide formulation.

CONCLUSION

This study reports the comparative compositional analysis of essential oil in leaf, flower and fruit of *Calotropis gigantea* for the first time with high benzyl alcohol (42.89%) and 4-vinylguaiacol (15.56 %) in flower, phytol content (17.94%) in leaf and 4-vinylguaiacol (3.86 %) in fruit essential oil as attention grabbing biochemical for health scientists as well as the fuel industry. Due to the presence of many biologically active molecules the EO or isolated molecules can be applied as a natural preservative, fuel additives and drugs including pesticides and bulk chemicals. Guaiacol is important building block chemicals in the range of traditionally produced molecules from fossil resources. The production/isolation of these chemicals products from *Calotropis gigantea* could help in exploring biobased chemical production to fulfill future energy chemical demands.

ACKNOWLEDGMENTS

REFERENCES

[1]Pari, K., Rao, P. J., Devakumar, C. and Rastogi, J. N., *J. Nat. Prod.*. **1998**, *61*, 102–104.

[2]Kadiyala, M., Ponnusankar, S. and Elango, K., *J. Ethnopharmacol.,* **2013**, *150*, 32–50.

[3]Srivastava, S. R., Keshri, G., Bhargavan, B., Singh, C. & Singh, M. M., *Contraception,* **2007**, *75*, 318–322.

[4]Meena, A. K., Yadav, A. & Rao, M. M., *Asian J. Trad. Med.,* **2011**, *6*, 45–53.

[5]Viji, R., Alaguraja, P., Mani, P., and S, Velavan., *Int. J. Res. Pure Appl. Microbiol.,* **2013**, *3*, 107–112.

[6]Sharma, J. K., Akhtar, M. S., Ameen, S., Srivastava, P. and Singh, G., *J. Alloys Compd.,* **2015**, *632*, 321–325.

[7]Bakry, F. A., *Pestic. Biochem. Physiol.,* **2009**, *95*, 159–165.

[8]Suresh, K. P., Chezhian, A., Senthil, R. P. and Sathiyapriya, J. *Bangladesh J. Pharmacol.,* **2012**, *7*, 1–5.

[9]Kumar, D. and Kumar, S., *Indian J. Res. Pharm. Biotechnol.,* **2015**, 218–235.

[10]Wang, C., Sun, J., Liu, X., Sudo, A. and Endo, T., *Green Chem.,* **2012**, *14*, 2799.

[11]Gao, D., Schweitzer, C., Hwang, H. T. & Varma, A., *Ind. Eng. Chem. Res.,* **2014**, *140416111530004*.

[12]Ashori, A. and Bahreini, Z., *J. Compos. Mater.,* **2009**, *43*, 1297–1304.

[13]Imteyaz, A. M., De, S., Dutta, S. and Saha, B., *RSC Adv.,* **2012**, *2*, 6890.

[14]Alam, M. I., De, S., Singh, B., Saha, B. and Abu-Omar, M. M. *Appl. Catal. A. Gen.,* **2014**, *486*, 42–48.

[15]Perricone, M., Arace, E., Corbo, M. R., Sinigaglia, M. and Bevilacqua, A. B., *Front. Microbiol.,* **2015**, *6*, 1–7.

[16]Turek, C. and Stintzing, F. C., *Compr. Rev. Food Sci. Food Safety.,* **2013**, *12*, 40–53.

[17]Bakkali, F., Averbeck, S., Averbeck, D. and Idaomar, M., *Food Chem. Toxicol.,* **2008**, *46*, 446–475.

[18]Rao, P. J., Mehrotra, K. N., *Indian J. Exp. Biol. Indian J. Exp. Biol.,* **1977**, *15*, 148– 150.

[19]Agrawal, A., Singh, N., Kannojia, P. and Garg, V. K., *IJAPR.,* **2011**, *2*, 613–620.

[20]Rastogi, P., Ram, M. B. N., *Compendium of Indian Medicinal Plants. CDRI, Lucknow and NISCAIR, New Delhi 5*, 2005.

[21]Kumar, G., Karthik L, B. R. K., *Int. J. Pharm. Sci. Rev. Res.,* **2010**, *4*, 141–144.

[22]Neto, M. C. L., F. B., Carlos., Thijan, V. N., Caldas, Germana F. R., Araujo, Alice V., Costa-Silva, J. H., Amorim, Elba L.C., Ferreira, Fabiano, Antonio, F. M., Wanderley, Almir G. *Brazilian J. Pharmacogn.,* **2013**, *23*, 913–919.

[23]Islam, M. T., Barros, M. V. O., Machado, Katia da Conceicao, Machado, Keylla da Conceicao, Amelia, Ana, Pergentino, Damiao, Mendes, Rivelilson, *Chem. Biol. Interact.,* **2015**, *240*, 60–73.

[24]Samira Jandoust, A. K., *J. Phys. Chem. Biophys.,* **2014**, *05*, 1–4.

[25]Mathew, S., Abraham, T. E. and Sudheesh, S., *J. Mol. Catal. B Enzym.,* **2007**, *44*, 48–52.

[26]Rao, B. R. R., Kaul, P. N., Syamasundar, K. V. and Ramesh, S., *Ind. Crops Prod.,* **2005**, *21*, 121–127.

[27]Devi, K. P., Nisha, S. A., Sakthivel, R. and Pandian, S. K., *J. Ethnopharmacol.,* **2010**, *130*, 107–115.

[28]Dua, V. K., Pandey, A. C., Singh, R., Sharma, V. P., Subbarao, S. K., *J. Appl. Entomol.,* **2003**, *127*, 509-11.

HYDROGEN BONDING AND ACTIVITY ANALYSIS OF CHOLANE CLASS OF STEROID DERIVATIVES

Sonia Sharma[a] and Rajni Kant[a]

Most of the crystallographic analysis that follows from structure determination involves interpretation of the molecular geometry and a working knowledge of a variety of intra- and intermolecular interactions based purely on geometrical considerations (distance and angle cut off criteria). In this paper, a total of fifty-nine structures of cholane derivatives have been chosen for the prediction of their biological activities and hydrogen bonding interaction analysis. Intermolecular interactions of the type X-H…A [X=C, O, N; A=O, Cl, N, Br] in all the structures have been computed and discussed primarily on the basis of distance-angle scatter for better understanding of molecular packing in cholane derivatives. In some structures, bifurcated hydrogen bonds have been observed. Solute-solvent/solvent-solute interactions have also been investigated to understand more complicated processes that occur for biomolecules in aqueous solution.

*Corresponding Authors
    Fax: +91 191 243 2051
    E-Mail: rkant.ju@gmail.com
[a]   X-ray Crystallography Laboratory, Department of Physics
    & Electronics, University of Jammu, Jammu Tawi -180
    006, India.

Introduction

In steroid biochemistry and pharmacology, the carbon skeleton or nucleus consisting of four-ring structure of which three are six-membered cyclohexane rings, one is five-membered cyclopentane ring and a side chain of five carbon atoms located at C17 position of steroid nucleus is regarded as a cholane molecule. Figure1 presents the representative illustration of cholane molecule.[1] The end product of cholesterol metabolism is bile acids which are dihydroxylated and trihydroxylated steroids with 24 carbon atoms i.e., cholane.[2]
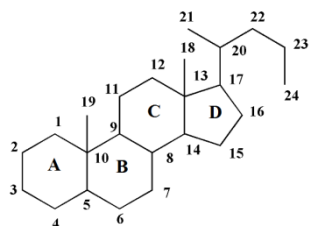

Figure 1. Basic cholane molecule (C24) with standard atomic numbering scheme

Bile acids, their conjugates, and bile salts are natural products that represent the 67% of the soluble components of bile. The most abundant mammalian bile acids are hydroxy derivatives of cholanoic acid and in humans, these consist mainly of cholic acid and chenodeoxycholic acid.[3] The bile acid group also includes conjugates of deoxycholic acid and lithocholic acid, commonly known as secondary bile acids, produced from cholic and chenodeoxycholic acids by intestinal bacteria

dehydroxylation.[4] Before excretion into the bile, acids are conjugate either with glycine or taurine to produce the bile salts.[5] These salts enter the small intestine where they facilitate lipid absorption.[6,7] Bile acids are largely reabsorbed from the intestine[8,9] and pass back to the liver in the enterohepatic circulation. Cholic and chenodeoxycholic (and its 7-hydroxy epimer ursodeoxycholic) acids have important pharmaceutical applications related to their ability to dissolve cholesterol gallstones and for the treatment of bile acid deficiency and cholestatic liver diseases.[10,11] Antiviral properties of bile acids have also been investigated.[12] Bile acids have potential medical applications as analgesics,[13] sensitizers of Gram negative bacterial to antibiotics,[14] and radiopharmaceuticals.[15]

The present work provides comprehensive information about biological activity, structural features and packing interactions/hydrogen bonding in cholane derivatives. Here, we have identified a series of fifty-nine derivatives of cholane from the literature (CSD). The chemical structure of each compound and its numbering is presented in Figure 2. The reference code, chemical name, chemical formula, molecular weight and published reference of each structure is presented in Table 1. [16-44]

Biological activity relationship

Biological activity is the result of chemical compound's interaction with biological entity. Any biologically active compound reveals wide spectrum of different effects. Some of them are useful in treatment of definite diseases but the others cause various side and toxic effects. Biological activity spectrum is defined as the "intrinsic" property of compound depending only on its structure and physico-chemical characteristics. Total complex of activities caused by the compound in biological entities is also called as the "biological activity spectrum of the substance".
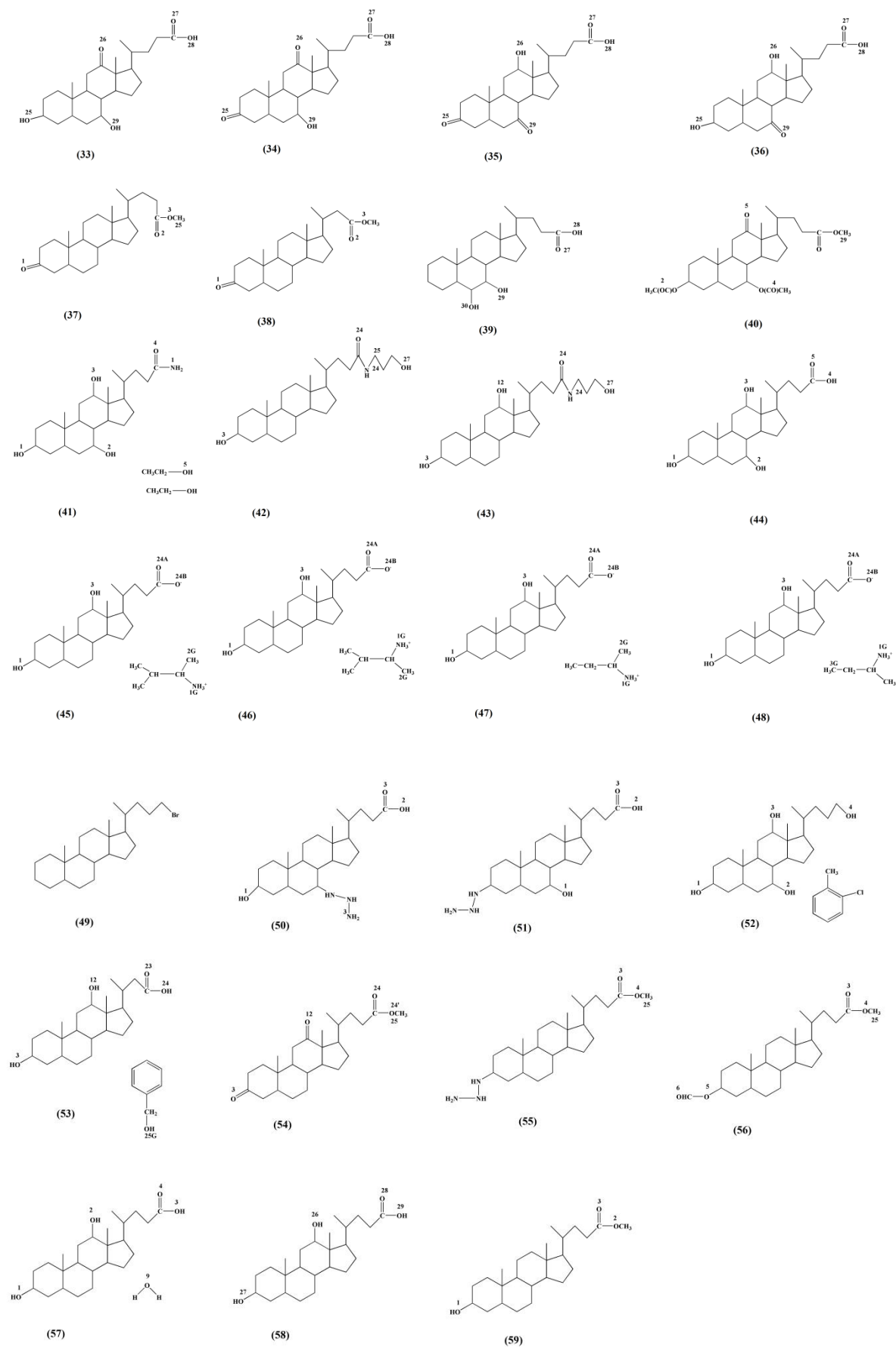
(1)

(2)

(3)

(4)

(5)

(6)

(7)

(8)

(9)

(10)

(11)

(12)

(13)

(14)

(15)

(16)

(17)

(18)

(19)

(20)

(21)

(22)

(23)

(24)

(25)

(26)

(27)

(28)

(29)

(30)

(31)

(32)

Figure 2. Chemical structures of molecules (**1-59**)

Table 1. CSD code, chemical name, chemical formula, molecular weight. and reference of molecules **1-59**

No.	Reference code	Chemical name	Chemical formula	MW, amu	Ref.,
M-1	ADIMAC	(+)-3,12-Dioxo-5β-cholanic acid	$C_{24}H_{36}O_4$	388.53	[16]
M-2	BUGJES01	3α,7α,12α-Trihydroxy-5β-cholan-24-oic acid monohydrate clathrate	$C_{24}H_{40}O_5.H_2O$	426.0	[17]
M-3	CELKOU	(-)-3,7-Dioxo-5β-cholanic acid	$C_2{}^4H_{36}O_4$	388.53	[18]
M-4	COYYAR	N-(2-Hydroxyethyl)-3α,7β-dihydroxy-5β-cholan-24-amide	$C_{26}H_{45}NO4$	435.63	[19]
M-5	COYYEV	N-(3-Hydroxypropyl)-3α,7β-dihydroxy-5β-cholan-24-amide	$C_{27}H_{47}NO4$	449.66	[19]
M-6	COYYIZ	N-(2-Hydroxyethyl)-3α,7α,12α-trihydroxy-5β-cholan-24-amide	$C_{26}H_{45}NO_5$	451.63	[19]
M-7	COYYOF	N-(3-Hydroxypropyl)-3α,7α,12α-trihydroxy-5β-cholan-24-amide	$C_{27}H_{47}NO_5$	465.66	[19]
M-8	COYZIA	Methyl 3α,7α,12α,15β-tetrahydroxy-5β-cholan-24-oate acetonitrile solvate	$C_{25}H_{42}O_6.C_2H_3N$	479.64	[20]
M-9	DADLEA	3β,12β-Dihydroxy-5β-cholan-24-oic acid	$C_{24}H_{40}O_4$	392.56	[21]
M-10	EBUYUV	(5S,8R,9R,10R,13S,14S,17R,20R)-5β-Cholan-24-yl chloride	$C_{24}H_{41}Cl$	365.02	[22]
M-11	EDIGAA	Methyl (20S, 22E)-3-β-acetoxy-5-α-chola-22-enoate	$C_{27}H_{42}O_4$	430.61	[23]
M-12	ERIMOH02	Cholic acid m-xylene p-xylene clathrate	$C_{24}H_{40}O_5.0.25C_8H_{10}.0.75C_8H_{10}$	514.74	[24]
M-13	ERIMOH03	Cholic acid m-xylene p-xylene clathrate	$C_{24}H_{40}O_5.0.12C_8H_{10}.0.87C_8H_{10}$	514.74	[24]
M-14	ERIMOH04	Cholic acid m-xylene p-xylene clathrate	$C_{24}H_{40}O_5.0.17C_8H_{10}.0.82C_8H_{10}$	514.74	[24]
M-15	ERIMOH05	Cholic acid m-xylene p-xylene clathrate	$C_{24}H_{40}O_5.0.37C_8H_{10}.0.61C_8H_{10}$	730.94	[24]
M-16	ERIPEA	Cholic acid m-xylene clathrate	$C_{24}H_{40}O_5.C_8H_{10}$	514.74	[24]
M-17	ERIPEA01(P)	Cholic acid m-xylene clathrate	$C_{24}H_{40}O_5.C_8H_{10}$	514.74	[24]
M-18	ERIPUQ(P)	Cholic acid p-xylene clathrate	$C_{24}H_{40}O_5.C_8H_{10}$	514.74	[24]
M-19	ERIPUQ01	Cholic acid p-xylene clathrate	$C_{24}H_{40}O_5.C_8H_{10}$	514.74	[24]
M-20	ERIQAX	Cholic acid m-xylene p-xylene clathrate	$C_{24}H_{40}O_5,0.56C_8H_{10}.0.45C_8H_{10}$	514.74	[24]
M-21	ERIQAX01	Cholic acid m-xylene p-xylene clathrate	$C_{24}H_{40}O_5.0.64C_8H_{10}.0.35C_8H_{10}$	514.74	[24]
M-22	EVUXEY	3α,12α-Dihydroxy-23-nor-5β-cholan-23-oic acid methanol clathrate	$C_{23}H_{38}O_4.CH_4O$	410.59	[25]
M-23	EVUZIE	Bis(3α,12α-Dihydroxy-23-nor-5β-cholan-23-oic acid) acetophenone clathrate	$2C_{23}H_{38}O_4.C_8H_8O$	877.25	[25]
M-24	EVUZOK	Bis(3α,12α-Dihydroxy-23-nor-5β-cholan-23-oic acid) 4'-methylacetophenone clathrate	$2C_{23}H_{38}O_4.C_9H_{10}O$	891.28	[25]
M-25	EVUZUQ	3α,12α-Dihydroxy-23-nor-5β-cholan-23-oic acid	$C_{23}H_{38}O_4$	378.55	[25]
M-26	EWABAF	3α,12α-Dihydroxy-23-nor-5β-cholan-23-oic acid toluene clathrate	$C_{23}H_{38}O_4.C_7H_8$	470.69	[25]
M-27	EWABEJ	3α,12α-Dihydroxy-23-nor-5β-cholan-23-oic acid o-xylene clathrate	$C_{23}H_{38}O_4.C_8H_{10}$	484.72	[25]
M-28	FABNUT	Ethyl cholate	$C_{26}H_{44}O_5$	436.0	[26]
M-29	FEBHUP02	3α,7β-dihydroxy-5β-cholan-24-oic acid	$C_{24}H_{40}O_4$	392.56	[27]
M-30	FOFCUZ	Methyl 11α-azido-3α,7α-diacetoxy-12-oxo-5β-cholan-24-oate	$C_{29}H_{43}N_3O_7$	545.66	[28]
M-31	FOFDAG	Methyl 11α-amino-3α,7α-diacetoxy-12-oxo-5β-cholan-24-oate	$C_{29}H_{45}NO_7$	519.66	[28]
M-32	FOHQEZ	Methyl 11β-azido-3α,7α-diacetoxy-12-oxo-5β-cholan-24-oate	$C_{29}H_{43}N_3O_7$	545.66	[28]
M-33	FOMPED	3α,7α-dihydroxy-12-oxo-5β-cholan-24-oic acid	$C_{24}H_{38}O_5$	406.54	[29]
M-34	FOMPIH	7α-hydroxy-3,12-dioxo-5β-cholan-24-oic acid	$C_{24}H_{36}O_5$	404.53	[29]
M-35	FOMPON	12α-hydroxy-3,7-dioxo-5β-cholan-24-oic acid	$C_{24}H_{36}O_5$	404.53	[29]
M-36	FONQEF	3α,12α-dihydroxy-7-oxo-5β-cholan-24-oic acid	$C_{24}H_{38}O_5$	406.54	[29]
M-37	GABGEW	Methyl 3-oxo-5β-cholan-24-oate	$C_{25}H_{40}O_3$	388.57	[30]

M-38	GIMRAW	(5R,8R,9S,10S,13R,14S,17R,20R)-3-oxo-5β-24-norcholanic acid	$C_{23}H_{36}O_3$	360.52	[31]
M-39	GOKCUF	6α,7α-Dihydroxy-5β-cholan-24-oic acid	$C_{24}H_{40}O_4$	392.56	[32]
M-40	GOKDIU01	3α,7α-diacetoxy-12-oxo-5β-cholan-24-oic acid methyl ester	$C_{29}H_{44}O7$	504.64	[33]
M-41	GUXDUY01	3α,7α,12α-Trihydroxy-5β-cholamide bis(ethanol) clathrate	$C_{24}H_{41}NO_4.2C_2H_6O$	499.73	[34]
M-42	HOLVOU	3α-Hydroxy-N-(3-hydroxypropyl)-5β-cholan-24-amide	$C_{27}H_{47}NO_3$	433.66	[35]
M-43	JAQFIR	N-(3-Hydroxypropyl)-3α,12α-dihydroxy-5β-cholan-24-amide	$C_{27}H_{47}NO_4$	449.66	[36]
M-44	JEYDEW01	3α,7α,12α-trihydroxy-5β-cholan-24-oic acid	$C_{24}H_{40}O_5$	408.56	[27]
M-45	KIBRAQ	(S)-3-Methyl-2-butylammonium (+)-deoxycholate	$C_5H_{14}NC_{24}H_{39}O_4$	479.72	[37]
M-46	KIBREU	(R)-3-Methyl-2-butylammonium (+)-deoxycholate	$C_5H_{14}NC_{24}H_{39}O_4^-$	479.72	[37]
M-47	KIBRIY	(S)-2-Butylammonium (+)-deoxycholate	$C_4H_{12}NC_{24}H_{39}O_4$	465.70	[37]
M-48	KIBROE	(R)-2-Butylammonium (+)-deoxycholate	$C_4H_{12}NC_{24}H_{39}O_4$	465.7	[37]
M-49	MOSWUN	(20R)-24-Bromo-5β-cholane	$C_{24}H_{41}Br$	409.48	[38]
M-50	MUTFAJ	7α-Azido-3α-hydroxy-5β-cholan-24-oic acid	$C_{24}H_{39}N_3O_3$	417.58	[39]
M-51	MUTFEN	3β-Azido-7β-hydroxy-5β-cholan-24-oic acid	$C_{24}H_{39}N_3O_3$	417.58	[39]
M-52	PEQKIH	Cholane-3,7,12,24-tetrol 1-chloro-2-methylbenzene solvate	$C_{24}H_{42}O_4.C_7H_7Cl$	521.18	[40]
M-53	SUQBUB01	3α,12α-Dihydroxy-23-nor-5β-cholan-23-oic acid benzyl alcohol clathrate	$C_{23}H_{38}O_4.C_7H_8O$	486.69	[25]
M-54	VIQPOB	(5α,8β,9β,10α,13α,14β,17α,20S)-Methyl 3,12-dioxocholan-24-oate	$C_{25}H_{38}O_4$	402.55	[41]
M-55	VODKEF	Methyl 3β-azido-5β-cholan-24-oate	$C_{25}H_{41}N_3O_2$	415.61	[42]
M-56	VODKIJ	Methyl 3β-formyloxy-5β-cholan-24-oate	$C_{26}H_{42}O_4$	418.60	[42]
M-57	YECPUT	3,12-Dihydroxycholan-24-oic acid hemihydrate	$C_{24}H_{40}O_4.0.5H_2O$	803.14	[43]
M-58	ZZZPNS01	3α,12β-Dihydroxy-5β-cholan-24-oic acid	$C_{24}H_{40}O_4$	392.56	[21]
M-59	ZZZPPO01	Methyl 3α-hydroxy-5β-cholan-24-oate	$C_{25}H_{42}O_3$	390.59	[44]

Table 2. P_a and P_i values for the molecules **1-59**

Mole cule	Anticarci-nogenic $P_a > P_i$	Dermatologic $P_a > P_i$	Antiinflam-matory, $P_a > P_i$	Antisebor-rheic, $P_a > P_i$	Antisecreto-ric, $P_a > P_i$	Antieczema-tic, $P_a > P_i$	Choleretic $P_a > P_i$
M-1	0.452>0.024	0.751>0.005	0.408>0.091	0.851>0.010	0.710>0.009	0.858>0.009	0.963>0.001
M-2	0.612>0.012	0.734>0.006	0.569>0.038	0.671>0.043	0.672>0.012	0.862 > 0.008	0.984>0.001
M-3	0.446>0.025	0.800>0.004	0.445>0.075	0.832>0.013	0.580>0.019	0.876 > 0.007	0.971>0.001
M-4	0.496>0.020	0.691>0.008	0.422>0.085	-	0.351>0.073	0.769 > 0.025	0.911>0.002
M-5	0.392>0.032	0.683>0.009	0.413>0.089	-	0.452>0.041	0.759 > 0.028	0.813>0.003
M-6	0.467>0.022	0.653>0.011	0.424>0.084	-	0.392>0.060	0.712 > 0.042	0.920>0.001
M-7	0.369>0.037	0.645>0.012	0.415>0.088	-	0.481>0.034	0.700 > 0.046	0.843>0.002
M-8	0.598>0.013	0.719>0.007	0.715>0.014	0.342 > 0.109	0.583>0.019	0.834 > 0.012	0.943>0.001
M-9	0.560>0.015	0.744>0.005	0.507>0.055	0.796 > 0.020	0.717 > 0.009	0.869 > 0.008	0.971>0.001
M-10	0.416>0.028	0.808>0.004	0.354>0.026	0.631 > 0.050	0.741 > 0.007	0.829 > 0.013	0.607>0.005
M-11	-	0.858>0.004	0.585>0.035	0.649 > 0.047	0.562 > 0.021	0.871 > 0.007	0.621>0.005
M-12	0.612>0.012	0.734>0.006	0.569>0.038	0.671 > 0.043	0.672 > 0.012	0.862 > 0.008	0.984>0.001
M-13	0.612>0.012	0.734>0.006	0.569>0.038	0.671 > 0.043	0.672 > 0.012	0.862 > 0.008	0.984>0.001
M-14	0.612>0.012	0.734 > 0.006	0.569>0.038	0.671 > 0.043	0.672 > 0.012	0.862 > 0.008	0.984>0.001
M-15	0.612>0.012	0.734 > 0.006	0.569>0.038	0.671 > 0.043	0.672 > 0.012	0.862 > 0.008	0.984>0.001
M-16	0.612 >0.012	0.734 > 0.006	0.569>0.038	0.671 > 0.043	0.672 > 0.012	0.862 > 0.008	0.984>0.001
M-17	0.612>0.012	0.734 > 0.006	0.569>0.038	0.671 > 0.043	0.672 > 0.012	0.862 > 0.008	0.984>0.001
M-18	0.612>0.012	0.734 > 0.006	0.569>0.038	0.671>0.043	0.672>0.012	0.862 > 0.008	0.984>0.001
M-19	0.612>0.012	0.734 > 0.006	0.569>0.038	0.671>0.043	0.672>0.012	0.862 > 0.008	0.984>0.001
M-20	0.612>0.012	0.734 > 0.006	0.569>0.038	0.671>0.043	0.672>0.012	0.862 > 0.008	0.984>0.001
M-11	-	0.858 > 0.004	0.585>0.035	0.649>0.047	0.562>0.021	0.871 > 0.007	0.621>0.005
M-21	0.612>0.012	0.734 > 0.006	0.569>0.038	0.671 > 0.043	0.672 > 0.012	0.862 > 0.008	0.984>0.001
M-22	0.483>0.021	0.718 > 0.007	0.441>0.076	0.823 > 0.015	0.689 > 0.011	0.857 > 0.009	0.962>0.001
M-23	0.483>0.021	0.718 > 0.007	0.441>0.076	0.823 > 0.015	0.689 > 0.011	0.857 > 0.009	0.962>0.001
M-24	0.483>0.021	0.718 > 0.007	0.441>0.076	0.823 > 0.015	0.689 > 0.011	0.857 > 0.009	0.962>0.001
M-25	0.483>0.021	0.718 > 0.007	0.441>0.076	0.823 > 0.015	0.689 > 0.011	0.857 > 0.009	0.962>0.001

M-26	0.483>0.021	0.718 > 0.007	0.441>0.076	0.823 > 0.015	0.689 > 0.011	0.857 > 0.009	0.962>0.001
M-27	0.483>0.021	0.718 > 0.007	0.441>0.076	0.823 > 0.015	0.689 > 0.011	0.857 > 0.009	0.962>0.001
M-28	0.554>0.015	0.713 > 0.007	0.599>0.032	0.445 > 0.083	0.704 > 0.010	0.865 > 0.008	0.983>0.001
M-29	0.651>0.011	0.768 > 0.005	0.570>0.038	0.724 > 0.033	0.632 > 0.015	0.888 > 0.005	0.980>0.001
M-30	-	0.585 > 0.017	-	-	-	0.735 > 0.034	0.855>0.002
M-31	0.465>0.023	0.616 > 0.014	0.334>0.133	-	0.380 > 0.064	0.764>0.027	0.909>0.002
M-32	-	-	-	-	-	0.735 > 0.034	0.855>0.002
M-33	-	-	-	-	0.617 > 0.016	0.849 > 0.010	0.988>0.001
M-34	-	-	-	-	-	0.838 > 0.011	0.988>0.001
M-35	-	-	0.457>0.071	0.761 > 0.026	-	0.838 > 0.011	0.988>0.001
M-36	0.575>0.014	0.731 > 0.006	0.445>0.075	0.751>0.028	0.612>0.017	0.849>0.010	0.988>0.001
M-37	0.377>0.035	0.799 > 0.004	0.507>0.055	0.813>0.017	0.690>0.011	0.843>0.011	0.922>0.001
M-38	0.392>0.032	0.792 > 0.005	0.438>0.078	0.898>0.004	0.704 > 0.010	0.872>0.007	0.938>0.001
M-39	0.471>0.022	0.750 > 0.005	0.425>0.083	0.629>0.050	0.515>0.027	0.897>0.005	0.920>0.001
M-40	0.511>0.018	0.687 > 0.009	0.507>0.055	0.520>0.069	0.575>0.020	0.827>0.013	0.971>0.001
M-41	0.401>0.030	0.691 > 0.008	0.457>0.070	0.447>0.083	0.408>0.055	0.744>0.032	0.934>0.001
M-42	0.356>0.040	0.693 > 0.008	0.353>0.121	-	0.499 > 0.030	0.769 > 0.025	0.740>0.003
M-43	0.336>0.046	0.655 > 0.011	0.357>0.118	-	0.536 > 0.024	0.712 > 0.042	0.771>0.003
M-44	0.612>0.012	0.734 > 0.006	0.569>0.038	0.671 > 0.043	0.672 > 0.012	0.862 > 0.008	0.984>0.001
M-45	0.466>0.023	0.759 > 0.005	0.491>0.060	0.792 > 0.021	0.642 > 0.014	0.844 > 0.010	0.934>0.001
M-46	0.466>0.023	0.759 > 0.005	0.491>0.060	0.792 > 0.021	0.642 > 0.014	0.844 > 0.010	0.934>0.001
M-47	0.466>0.023	0.759 > 0.005	0.491>0.060	0.792 > 0.021	0.642 > 0.014	0.844 > 0.010	0.934>0.001
M-48	0.466>0.023	0.759 > 0.005	0.491>0.060	0.792 > 0.021	0.642 > 0.014	0.844 > 0.010	0.934>0.001
M-49	0.338>0.045		-	0.537 > 0.066	-	0.829 > 0.013	0.622>0.005
M-50	0.305>0.056	0.658 > 0.010	-	-	0.304 > 0.089	0.840 > 0.011	0.814>0.003
M-51	-	0.652 > 0.011	0.310>0.152	-	0.327 > 0.081	0.821 > 0.014	0.817>0.003
M-52	0.542>0.016	0.741 > 0.005	0.569>0.039	0.496 > 0.073	0.606 > 0.017	0.793 > 0.020	0.952>0.001
M-53	0.367>0.037	0.741 > 0.005	0.403>0.094	0.784 > 0.022	0.627 > 0.015	0.799 > 0.019	-
M-54	0.367>0.037	0.741 > 0.005	0.403>0.094	0.784 > 0.022	0.627 > 0.015	0.799 > 0.019	0.932>0.001
M-55	-	0.658 > 0.010	-	-	0.345 > 0.075	0.779 > 0.023	0.510>0.008
M-56	-	0.667 > 0.010	-	0.338 > 0.110	0.430 > 0.048	0.819 > 0.015	0.771>0.003
M-57	0.560>0.015	0.744 > 0.005	0.507>0.055	0.796 > 0.020	0.717 > 0.009	0.869 > 0.008	0.971>0.001
M-58	0.560>0.015	0.744 > 0.005	0.507>0.055	0.796 > 0.020	0.717 > 0.009	0.869 > 0.008	0.971>0.001
M-59	0.525>0.017	0.757 > 0.005	0.506>0.055	0.733 > 0.031	0.646 > 0.014	0.861 > 0.008	0.945>0.001

Biological-activity spectrum provides the rationale for predicting biological activity types for different compounds. Any component of this spectrum of a given compound is assumed to be detectable under suitable experimental conditions. By using a qualitative representation of biological activity, it is possible to compare and mix activity data for obtaining robust quantitative models.[45] Multilevel Neighbourhoods of Atoms (MNA) descriptors are helpful in describing the crystal structures.[46] These descriptors are successfully applied for predicting the biological activity in drug-like compounds.[47] The MNA descriptors represent various structure property relationships including many types of biological activity,[48] carcinogenicity,[49] drug-likeness,[50]etc.

The three-dimensional (3D) coordinate data of all the compounds have been selected as an input for the PASS software to predict the bioactivity relationship.[49] The biological activity spectra have been correlated empirically on the basis of structure-activity relationship which provides different P_a (probability of activity) and P_i (probability of inactivity) values. Based on statistics of MNA descriptors for active and inactive compounds, two probabilities have been calculated for each activity: P_a- probability of the compound being active and P_i- probability of the compound being inactive. Influence of these descriptors can be positive (if they are found in compounds with particular activity) or negative (if they are found in compounds without the particular activity) or even neutral. The P_a and P_i values for the molecule (1-59) have been computed by the pass

software[52] and are given in Table 2. It is quite interesting to note that most of the cholane derivatives possess high *choleretic, dermatologic, antieczematic, antisecretoric* and *antiseborrheic* activity while *anti-inflammatory* and *anticarcinogenic* activity is not much significant.

Hydrogen Bonding

Carbon forms weak hydrogen bonds like C-H…O which is ubiquitous and occurs in most molecular crystals[53,54] Hydrogen bonding is directional, mostly noncovalent interaction which is fundamental element of chemical structure[55] and reactivity.[56] On the basis of some studies which have been carried out by various workers on hydrogen bonding,[54, 57-58] we got interested in the analysis of various kinds of hydrogen bonded interactions present in cholane derivatives (**1-59**) and the study has been carried out to (i) generate H-bonds by calculating the *d*, *D* and *θ* values for the compounds which are listed in CCDC data, (ii) know whether C-H…O or O-H…O hydrogen bonding is predominant in this class of steroids, (iii) make a small compendium of hydrogen bonding on a comparative graphical scale. The number of hydrogen donors as well as acceptors and comparative data of intermolecular hydrogen bonds of the type O-H…O, C-H…O, N-H…O, C-H…Cl, C-H…N, C-H…Br in molecule (1-59) are presented in Table 3. Different kind of intermolecular hydrogen bonds viz. O-H…O, C-H…O, N-H…O, C-H…Cl, C-H…N, C-H…Br have been observed.

Table 3. Geometry of C-H...O, O-H...O, N-H…O, C-H…Cl, C-H…N and C-H...Br intermolecular interactions.

Molecule [Number of donors and acceptors]	Intermolecular interactions, X-H...A	H...A(Å) d	X...A(Å) D	X-H...A(Å) θ
M-1 ADIMAC Donors=10 Acceptors =6	O4-H4AC...O3'	1.841	2.672	169.7
	O4'-H4BC...O3	1.814	2.654	179.2
	O2-H2AA...O1'	2.704	3.186	110.3
	C23-H23C...O3'	2.385	3.327	158.8
	C1-H1AA...O1	2.645	3.561	153.8
	C19-H19A...O1	2.527	3.419	151.3
	C6'-H6BB...O2	2.717	3.516	138.0
	C19'-H19E...O2'	2.653	3.632	177.7
	C6'-H6BA...O2'	2.495	3.311	139.5
	C8'-H8BA…O2'	2.604	3.399	136.3

The key structural feature distinguishing the hydrogen bond from the other non-covalent interactions is its preference for linearity.[59] A better way to analyse preferences is to draw d-θ and D-θ scatter plots. The plots include all contacts found in molecules (1-59) with $d <$ 2.915Å and D<3.834 Å at any occurring angle. The graphical projections of d-θ [d (H...A) against θ (X-H...A)] and D-θ [D (X...A) against θ (X-H...A)] scatter plots have been made for intermolecular interactions which are shown in Figure 3a and 3b. The following observations have been made:
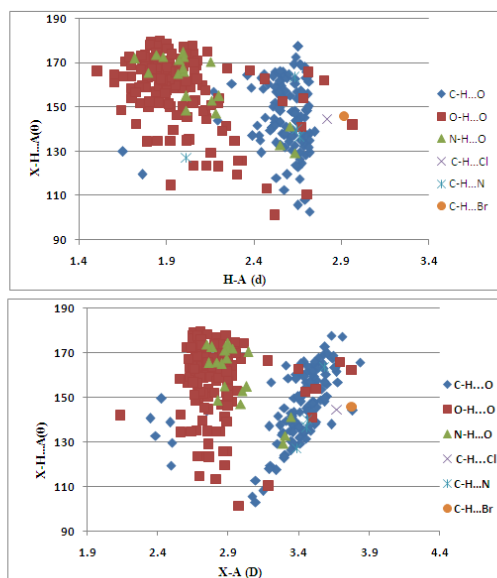

Figure 3 (a) d-θ scatter plot for intermolecular C-H...O, O-H...O, N-H...O, C-H...Cl, C-H...N and C-H...Br. (b) D-θ scatter plot for intermolecular C-H...O, O-H...O, N-H...O, C-H...Cl, C-H...N and C-H...Br.

The density of spots for d(H...A) [= 2.5-2.75 Å] and D (X...A) [= 3.30-3.65 Å] is predominant [θ (X-H...A) range ~130-170°] in case of C-H...O hydrogen bonds.

The density of spots for O-H...O intermolecular hydrogen bonds is quite high in a given range of values for d (H...A) =1.80-2.25 Å and D (X...A) =2.60-2.95 Å and θ (X-H...A)=150–180°.

The relative frequency of occurrence of various types of O-H...O, C-H...O, N-H…O, C-H…N, C-H…Cl and C-H...Br intermolecular hydrogen bonds is 48.85, 42.95, 6.23, 1.31, 0.32 and 0.32 %,   respectively and it is shown in Figure 4.
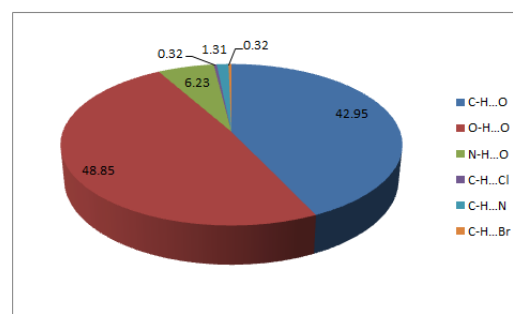

Figure 4. Relative frequency of occurence (in%) for various types of intermolecular hydrogen bonding.

Densely populated clusters at short distances and fairly linear angles have been found and each point in these clusters represents a hydrogen bond. Plots analogous to these figures exist in the literature for other kinds of hydrogen bonds, such as O-H...O, C-H...O, etc.[60,61] Similar features (preference for linearity) have been depicted by these plots which indicate that the angular characteristics of all kinds of hydrogen bonds are related. On comparison of the frequency of contacts from H(C) to O, N, Cl and Br, it has been concluded that H(C) atoms have a statistical preference for contacts to 'O' rather than 'N', 'Cl' or 'Br' atoms. Thus, with oxygen as an acceptor, the frequency of occurrence of C-H...O hydrogen bond becomes very high (42.95 % in the present case). In all the molecules (**1-59**), the C atoms act as donors but not as acceptors in all the bonds. Most of the C-H...O contacts have distance d (H...O) less than 2.7 Å and based on the criterion that the van der Waals distance should be <2.7 Å, it was regarded as a certain indication of hydrogen bonding.

Due to long range character of hydrogen bond and a pronounced softness of the angle at H, donors may interact simultaneously with more than one acceptor, thus forming bifurcated hydrogen bond (X-H...(A1,A2)). Here, X atom is referred to as bifurcated donor Sometimes, acceptors may interact simultaneously with more than one donor (X1,

X2-H...A). Atom A here is a bifurcated acceptor. In some cases, an atom can act both as donor as well as acceptor simultaneously. Bifurcated hydrogen bonds are commonly observed in O-H…O and N-H…O hydrogen bonded structures.[62] They are also observed in C-H…O/N patterns. In the present study, bifurcated or trifurcated hydrogen bonds have been observed mostly in C-H…O and O-H…O hydrogen bonded structures and in almost all the structures (with *Z'*=1, 2 and 3), with oxygen acting as a bi or tri or multifurcated hydrogen bond acceptor.

The solute-solvent intermolecular interactions and the effect of solvent on the properties of organic and biological molecules has been successfully described by various workers using different and complementary theoretical models.[63-65] In this direction the investigation as carried out on the solvation mechanism[66] and the specific role of the solute-solvent interactions could be used as a tool for supramolecular structures.[67,68] The specific C-H…O hydrogen bonds between solute and solvent play an important role in solid state chemistry.[69] In the present work we have come across a few cases where solute-solvent interactions have been observed. Some of the prominent solute–solvent interactions as obtained in the present case are: [O2-H38…O6(W), O5-H40…O6(W), C14-H17…O6(W),C9-H13,O6][M-2], [O2'-H75…O9][M-23], [O2-H37…O9][24], [N1-H40…O5][41], and the solvent-solute interactions are: [C31-H31B…O3][M-19], [O5-H42…O2][M-22], [C54-H82…O3][M-23], [NIG-H15…O24A, NIG-H15…O24B][M-45], [NIG-H26…O24A, NIG-H26…O24B][M-46], [NIG-H56…O3, NIG-H54…O24A, NIG-H54…O24B][M-47], [NIG-H143…O3, NIG-H1G1…O24A][M-48], [O25G-H46…O12][M-53] respectively. A representative view of such an interaction in molecule M-2 is shown in Figure 5.
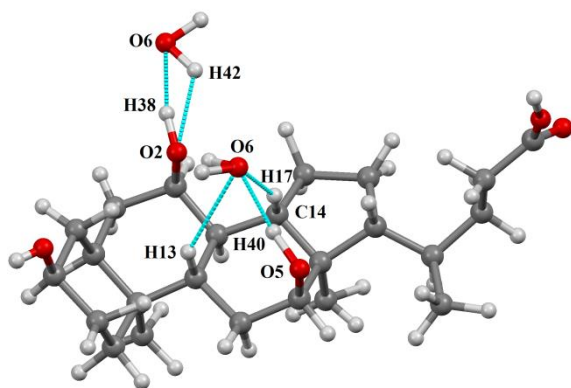

Figure 5. Solute-solvent/solvent-solute interactions in molecule (M-2).

Conclusion

The relationship between X-ray crystallography and structure- activity relationships have high affinity to indicate the drug-likeness and conserved arginine in the binding site for the steroid receptors. The molecules in the unit cell are linked by C-H…O/O-H…O interactions and most of these are associated through the keto and the

hydroxyl group located at C3/C12 position of the cholane derivatives. These secondary interactions help in understanding the stacking of molecules in the unit cell as supramolecular entity. It is depicted that unusual substitution with the basic steroid moiety/nucleus may change the biological activity of the molecule.

References

[1]Makin, H. L. J., *Biochemistry of Steroid Hormones*, Oxford: Blackwell Scientific Publications, **1975**, 5.

[2]Noponen, V., Nonappa, V., Lahtinen, M., Valkonen, A., Salo, H., Kolehmainen, E., Sievanen, E., *Soft Matter*, **2010**, *6*, 3789.

[3]Bortolini, O., Fantin, G., Fogagnolo, M., *Chirality*, **2010**, *22*, 486.

[4]Bortolini, O., Medici, A., Poli, S., *Steroids*, **199**7, *62*, 564.

[5]Makin, H. L. J., *Biochemistry of Steroid Hormones,* Oxford: Blackwell Scientific Publications, **1975**, 43.

[6]Holt, P. R., *Arch. Int. Med.,* **1972,** *130*, 574.

[7]Hoffman, A. F., Mekjian, H. S., In: *The Bile Acids* (Nair P. P & Kritchevsky D, eds), Plenium Press, New York, **1972**, *2*, 103.

[8]Dietschy, J. M., *J. Lipid Res*., **1968**, *19,* 297.

[9]Lack, L., Weiner, I. M., In : *The Bile Acids* (Nair P. P & Kritchevsky D, eds), , Plenium Press, New York, **1973**, *2*, 33.

[10]Paumgartner, G., Stiehl, A., Gerok, W., *Trends in bile acid research.* Dordrecht: Kluwer Academic Publishers, **1989**.

[11]Enhsen, A., Kramer, W., Wess, G., *Drug Discov. Today*, **1998**, *3*, 409.

[12]Berlati, F., Ceschel, G., Clerici, C., Pellicciari, R., Roda, A., Ronchi, C., *Use of bile acids as antiviral agents. WO 94/00126*, **1994.**

[13]Ruff, M. R., Hill, J. M., Kwart, L. D., Pert, C. B., *US 5446026*, **1995**.

[14]Li, C., Budge, L. P., Driscoll, C. D., Willardson, B. M., Allman, G. W., Savage, P. B., *J. Am. Chem. Soc*., **1999**, *121*, 931.

[15]Campazzi, E., Cattabriga, M., Marvelli, L., Marchi, A., Rossi, R., Pieragnoli, M.R., Fogagnolo, M., *Inorg. Chim. Acta,* **1999**, *286*, 46.

[16]Kikolski, E. M., Davison, M., Lalancette, R. A., Thompson, H. W., *Acta Crystallogr., Sect. E. Struct. Rep. Online,* **2006**, *62*, o2641.

[17]Shibakami, M., Tamura, M., Sekiya, A., *J. Am. Chem. Soc.,* **1995**, *117*, 4499.

[18]Kikolski, E. M., Lalancette, R. A., Thompson, H. W., *Acta Crystallogr., Sect. C: Cryst. Struct. Commun.,* **2006**, *62*, o394.

[19]Valkonen, A., Lahtinen, M., Kolehmainen, E., *Steroids,* **2008**, *73,* 1228.

[20]Al-Aboudi, A., Mohammad, M.Y., Haddad, S., Al-Far, R., Choudhary, M. I., Atta-ur-Rahman, *Steroids,* **2009**, *74,* 483.

[21]Jover, A., Meijide, F., Soto, V. H., Tato, J. V., Nunez, E. R., Ton-Nu, H. T., Hofmann, A. F., *Steroids,* **2004**, *69,* 379.

[22]Cox, P. J., Nahar, L., Turner, A. B., *J. Chem. Res.,* **2001**, 162.

[23]Shingate, B. B., Hazra, B. G., Pore, V. S., Gonnade, R. G., Bhadbhade, M. M., *Tetrahedron,* **2007**, *63,* 5622.

[24]Nakano, K., Mochizuki, E., Yasui, N., Morioka, K., Yamauchi, Y., Kanehisa, N., Kai, Y., Yoswathananont, N., Tohnai, N., Sada, K., Miyata, M., *Eur. J. Org. Chem.,* **2003**, 2428.

[25]Kato, K., Sugahara, M., Tohnai, N., Sada, K., Miyata, M., *Eur. J. Org. Chem.,* **2004**, 981.

[26]Nonappa, Lahtinen, M., Behera, B., Kolehmainen, E., Maitra, U., *Soft Matter,* **2010**, *6,* 1748.

[27]Nonappa, Lahtinen, M., Ikonen, S., Kolehmainen, E., Kauppinen, R., *Cryst. Growth Des.,* **2009**, *9,* 4710.

[28]Salunke, D. B., Hazra, B. G., Gonnade, R. G., Bhadbhade, M. M., Pore, V. S., *Tetrahedron,* **2005**, *61,* 3605.

[29]Bertolasi, V., Ferretti, V., Pretto, L., Fantin, G., Fogagnolo, M., Bortolini, O., *Acta Crystallogr., Sect.B: Struct. Sci.,* **2005**, *61,* 346.

[30]Virtanen, E., Valkonen, A., Tamminen, J., Kolehmainen, E., *J. Mol. Struct.,* **2003**, *650,* 201.

[31]Dufort, M. D., Davison, M., Lalancette, R. A., Thompson, H. W., *Acta Crystallogr., Sect. C: Cryst. Struct. Commun.,* *2007*, *63,* o646.

[32]Bertolasi, V., Ferretti, V., Fantin, G., Fogagnolo, M., *Z. Kristallogr.,* **2008**, *223,* 515.

[33]Salunke, D. B., Hazra, B. G., Gonnade, R. G., Pore, V. S., Bhadbhade, M. M., *J. Mol. Struct.,* **2008**, *892,* 246.

[34]Yoswathananont, N., Sada, K., Nakano, K., Aburaya, K., Shigesato, M., Hishikawa, Y., Tani, K., Tohnai, N., Miyata, M., *Eur. J. Org. Chem.,* **2005**, 5330.

[35]Valkonen, A., Koivukorpi, J., Lahtinen, M., Kolehmainen,E., *Acta Crystallogr., Sect. E: Struct. Rep. Online,* **2009**, *65,* o650.

[36]Valkonen, A., Lahtinen, M., Virtanen, E., Kaikkonen, S., Kolehmainen, E., *Biosens. Bioelectron.,* **2004**, *20,* 1233.

[37]Jacobs, A., Bathori, N. B., Nassimbeni, L. R., Sebogisi, B. K., *CrystEngComm.,* **2013**, *15,* 931.

[38]Ketuly, K. A., Hadi, A. H. A., Ng, S. W., *Acta Crystallogr., Sect.E: Struct. Rep. Online,* **2009**, *65,* o1124.

[39]Felici, M., Carballada, P. C., Smiths, J. M., Nolte, R. J. M., Williams, R. M., Cola, L. D., Feiters, M. C., *Molecules,* **2010**, 15, 2039.

[40]Liu, W. T., Kin, Y., Nakano, K., Hisaki, I., Tohnai, N., Miyata, M., *Chem.Lett.,* **2013**, *42,* 143.

[41]Katona, B. W., Rath, N. P., Anant, S., Stenson, W. F., Covey, D. F., *J. Org. Chem.,* **2007**, *72,* 9298.

[42]Valkonen, A., Lahtinen, M., Tamminen, J., Kolehmainen, E., *J. Mol. Struct.,* **2008**, *886,* 197.

[43]Singh, K. S., Kaminsky, W., *Nat. Prod. Commun.,* **2011**, *6,* 1237.

[44]Virtanen, E., Valkonen, A., Tamminen, J., Kolehmainen, E., *J. Mol. Struct.,* **2003**, *649,* 207.

[45]Verma, R., Jasrotia, D., Chand, B., *J. Chem. Crystallogr.,* **2008,** *38,* 567.

[46]Filimonov, D. A., Poroikov, V. V., Borodina, Y., Gloriozova, T., *J. Chem. Inf. Comput. Sci.,* **1999**, *39,* 666.

[47]Rajnikant, Dinesh and Chand, B., *Ind. J. Biochem, Biophys.,* **2007**, *44,* 458.

[48]Poroikov, V. V., Filimonov, D. A., *Computer- assisted predictions of biological activity in search for and optimization of new drugs,* Iridium Press, Moscow, **2001**, 149.

[49]Suchkov, A. P., Filimonov, D. A., Stepanchikova, A. V., Poroikov, V. V., *Environ. Res.,* **2001**, *12,* 327.

[50]Anzali, S., Barnickel, G., Cezanne, B., Krug, M., *J. Med. Chem.,* **2001**, *44,* 2432.

[51]Poroikov, V. V., Filimonov, D. A., Ihlenfeldt, W. D., Gloriozova, T. A., Lagunin, A. A., Borodina, Y., Stepanchikova, A. V., Nicklaus, M. C., *J. Chem. Inf. Comput. Sci.,* **2003**, *43,* 228.

[52](a)Geronikaki, A., Druzhilovsky, D,, Zakharov, A., Poroikov, V., *SAR and QSAR Environ Res.,* **2008**, *19,* 27. (b)Filz, O. A., Poroikov, V. V., *Russian Chem Rev.,* **2012**, *81*(2), 158.

[53]Desiraju, G. R., *Acc. Chem. Res.,* **1991**, *24,* 270.

[54]Steiner, T., *Crystallogr. Rev.,* **1996**, *6,* 1.

[55]Murrel, J. N., Randi, M., Williams, D. R., *Proc. Roy. Soc. London Ser A,* **1965**, *284,* 566.

[56]Kojic-Prodic, B., Molcanov, K., *Acta Chim. Slov.,* **2008**, *55,* 692.

[57]Steiner, T., *Acta Cryst B,* **1998**, *54,* 456.

[58]Desiraju, G.R., Steiner, T., *The weak hydrogen bond in structural chemistry and biology.* Oxford University Press Inc., New York, **1999**.

[59]Steiner,T., *Angew. Chem., Int. Ed. Engl.,* **2002**, *41,* 48.

[60]Steiner, T., Saenger, W., *J. Am. Chem. Soc.,* **1992**, *114,* 10146.

[61]Steiner,T., Saenger, W., *Acta Cryst B,* **1992**, *48,* 819.

[62]Jeffery, G. A., Saenger, W., *Hydrogen bonding in biological structures.* Springer-Verlag, Berlin, 1991.

[63]Kollman, P., *Chem. Rev.,* **1993**, *93,* 2395.

[64]Cramer, C. J., Truhlar, D. G., *Chem. Rev.,* **1999**, *99,* 2161.

[65]Baldridge, K. K., Jonas, V., Bain, A. D., *J. Chem. Phys.,* **2000**, *113,* 7519.

[66]Allen, M. P., Tildesley, D. J., *Computer simulation of liquids,* Oxford University Press, New York, **1987.**

[67]Coutinho, K., Canuto, S., Zerner, M. C., *J. Chem. Phys.,* **2000**, *112,* 9874.

[68]Canuto, S., Coutinho, K., Trzesniak, D., *Adv. Quantum Chem.,* **2002**, *41,*161.

[69]Desiraju, G. R., Steiner, T., *The weak hydrogen bond in structural chemistry and biology.* Oxford University Press Inc., New York, **1999**, 116.